# Multiphase CFD Simulation for Performance Estimation of Forced Feed Venturi Scrubber Using Euler-Lagrange Method


**Attaullah**

**NUST201463879MSCME67814F**

**This work is submitted as a MS thesis in partial fulfilment of the requirement for the degree of**

**(M.S in Chemical Engineering)**

**Supervisor Name: Dr. Bilal Khan Niazi**

**School of Chemical and Materials Engineering (SCME)**

**National University of Sciences and Technology (NUST),**

**H-12 Islamabad, Pakistan**

**October, 2017**

# *Dedication*

*This thesis is dedicated to my parents, siblings*

## Acknowledgments

Praise is due to **ALLAH** whose worth cannot be described by speakers, whose bounties cannot be counted by calculators, whom the height of intellectual courage cannot appreciate, and the divings of understanding cannot reach; He for whose description no limit has been laid down, no eulogy exists, no time is ordained and no duration is fixed. Countless salutation upon **"HOLY PROPHET HAZRAT MUHAMMAD (S.A.W.W.)".**

I would like to acknowledge and express my sincere gratitude to my research **supervisor, Dr. Bilal Khan Niazi** for his endless support, supervision and affectionate guidance to steer me in the right direction whenever he thought I needed it. I would also like to extend my gratitude to my Guidance committee members; **Dr. Arshad Hussain** and **Dr. Majid Ali & Dr. Iftikhar** for their valuable suggestions and guidance.

I would also like to thank **Dr. Arshad Hussain** (Principal, School of Chemical and Materials Engineering) and **Dr. Abdul Qadir Malik** (HOD, Department of Chemical Engineering) for providing a research oriented platform to effectively utilize my skills in accomplishing this research work.

In the end, I must express my very profound gratitude to my parents for providing me with unfailing support and continuous encouragement throughout my years of study and through the process of researching and writing this thesis. This accomplishment would not have been possible without them.

*Atta ullah*

# Abstract

The adverse and severe effects of particulates and toxic gasses on human health and environment demand an efficient scrubbing system which reduces the toxicity of the pollutants to a desirable value. Venturi scrubber is widely employed to abate the pollutant concentration because of their high removal efficiency. For an accurate and efficient design of venturi scrubber, the complex fluid dynamic behavior inside the venturi scrubber should be analyzed. The present Multiphase Euler-Lagrange CFD study deals with the developed three phase model to predict pressure drop and collection efficiency. The continuous phase is resolved in the Eulerian frame of reference by solving the Navier Stokes equation while dust and droplet are treated in Lagrangian framework through DPM model. The model takes into account the turbulence through the realizable k-**ε** model, TAB model for droplet secondary breakup and drag coefficient is modeled through dynamic and spherical drag laws for dust and droplet. Effect of design parameters like throat gas velocity, droplet diameter and L/G ratio (L/G ratio) on venturi scrubber performance are investigated. Results of pressure drop predicted by this model agree well with experimental data and Open FOAM simulation. Collection efficiency predicted by this model using Calvert and Mohebbi equations concur well with experimental data. It is concluded that the efficiency calculation by Mohebbi equation presents less relative error as compared to Calvert equation with respect to experimental data.

# Nomenclature

| | |
|---|---|
| A | Area ($m^2$) |
| C | Concentration |
| $C_{1\varepsilon}, C_{2\varepsilon}$ | Constants of k-$\varepsilon$ model |
| F | Force (N) |
| G | Generation ($kg/m.s^3$) |
| G | Gravity ($m/s^2$) |
| K | Turbulent kinetic energy (*m2/s2)* |
| P | Pressure (Pascal) |
| $R_e$ | Reynolds number |
| U | Velocity (m/s) |
| Q | Volumetric flow rate ($m^3/s$) |
| D | Diameter (m) |
| $u_i$ | Instantaneous velocity vector of gas velocity |
| $v_i$ | Instantaneous velocity vector of droplet velocity |
| $H_D$ | Volume fraction of droplet |
| $M_d$ | Mass of dispersed phase (kg) |
| $C_D$ | Drag Coefficient |
| $n_p$ | Number concentration of dust particles |
| R | Radius (m) |
| S | Source term |
| T | Time (s) |

| | |
|---|---|
| W | Mass flow rate (kg/s) |
| $W_e$ | Weber number |
| $V_d$ | Dispersed phase volume fraction ($m^3$) |
| $V_c$ | Continuous phase volume fraction ($m^3$) |
| X | Quality |
| Z | Loading |
| $x_i, x_j$ | Gas field coordinates |
| Y | Distortion |

**Greek Words**

| | |
|---|---|
| $\boldsymbol{\rho}$ | Density ($kg/m^3$) |
| $\boldsymbol{\eta}$ | Inertial impaction efficiency |
| $\boldsymbol{\lambda_f}$ | Friction factor |
| $\boldsymbol{\eta_i}$ | Target efficiency |
| $\Psi_c'$ | Stokes number |
| M | Gas viscosity (kg/m.s) |
| $\boldsymbol{\alpha_d}$ | Volume fraction of dispersed phase |
| $\boldsymbol{\tau}$ | Viscous stress tensor |
| $\boldsymbol{\sigma}$ | Surface tension (N/m) |
| $\boldsymbol{\varepsilon}$ | Turbulent Dissipation Energy ($m^2/s^3$) |

**Abbreviations**

| | |
|---|---|
| CFD | Computational Fluid Dynamics |
| VOF | Volume of fluid |
| St | Stokes |

| | |
|---|---|
| CAB | Cascade atomizing and breakup |
| DPM | Discrete phase model |

**Subscript or Superscript**

| | |
|---|---|
| B | Buoyancy (N) |
| G, g | Referring to Gas |
| T | Throat |
| T | Target |
| C | Continuous |
| S | Solid |
| d, d | Droplet, dispersed |
| L | Liquid |
| LE | Entrainment liquid |
| D | Drag |
| M | Mixture |
| K | Kth continuous phase |
| P | Particle |

# Table of Contents

# List of Figures

# List of Tables

# Chapter-1

# Introduction

With the advent of modern technology and industrial revolution, control of particulate emissions from the industrial processes is the key issue for the past several decades. The yield of particulate emissions is a source of concern for both industry itself and the human health as well. Due to stringent environmental regulations, an effective and economical design of gas cleaning devices is of paramount importance. Micron and submicron particles should be effectively removed as they can cause severe health issues in the form of respirable dust. To abate the toxicity of particle laden gas, an efficient cleaning and pollution control equipment is needed.

Micron size particulate matter like dust, mist and fumes are the results of the industrial process which are as follows [1]:

a) Power stations
b) Coal industry
c) Coal gas industry
d) Chemical industry
e) Mineral Earths and salt processing
f) Metallurgical Industry

The prominent control equipment's like cyclone separators, electrostatic precipitators and scrubbers for the abatement of particulates from the moving gas streams operates on the basis of cyclonic, electrostatic and inertial principles. Equipment based on inertial principles have been a best choice for such applications. Venturi scrubber is on the top of the list in this category [1].

## 1.1 Venturi scrubber

The venturi scrubber is an effective pollution control system for the abatement of particulates as well as toxic gaseous pollutants. As one of the most effect pollution control technology, the merits of selecting venturi scrubber are as follows:

a) Lower initial investment costs compared to its competitors.
b) Compact volume and no moving parts.
c) Adequate for handling hot, corrosive and wet gases.

A venturi scrubber is typically divided into convergent, throat and divergent section (see Figure 1.1). The cross section could be rectangular or circular.

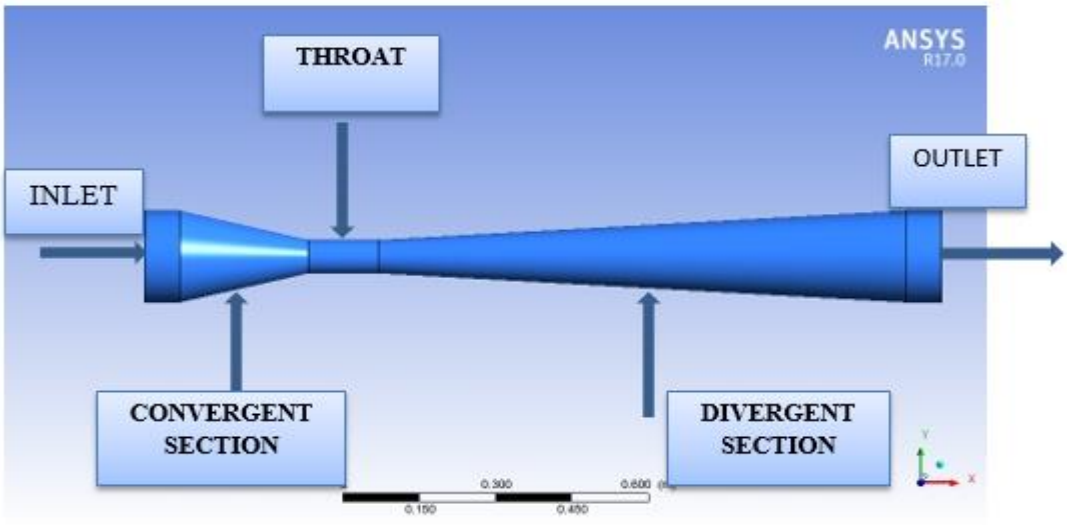


**Figure 1-1 Venturi scrubber**

The particulate laden gas enters the venturi scrubber through the inlet and accelerates in the convergent section to the desired throat velocity. Liquid injection is carried out in two ways: 1) Injection approach in which liquid is sprayed directly into the venturi throat and 2) wetted approach in which liquid injection as a film followed by atomization due to drag force [2]. Particulates moving with high speed are collected by these droplets which act as an inertial collector and moving with a low velocity. The diffuser section is designed to recover the pressure lost during all this process [3].

The performance estimation variables of venturi scrubber are collection efficiency and pressure drop. Following are the design parameters that can be considered in estimating the performance of venturi scrubber.

a) Aerodynamic particle size
b) L/G ratio (loading)
c) Penetration length of liquid
d) Liquid droplet size distribution
e) Throat coverage by liquid
f) Venturi scrubber geometry

Numerous efforts to calculate the particulate collection efficiency theoretically has been made by several investigators like Calvert [4] and Boll [5]. The models were based on the assumption of uniform distribution of liquid drops in the throat section.

Fine particles are collected in the venturi scrubber at the expense of the high energy consumption required to accelerate the particle laden streams to the desired throat velocity. Components that contributes to the total pressure drop are [6]:

a) Acceleration pressure drop (gas).
b) Acceleration pressure drop (droplets).
c) Momentum change of the film / Acceleration pressure drop (film)
d) Frictional pressure drop.
e) Gravitational (static) pressure drop.

Pressure drop as an important performance parameter has been widely studied and predicted by several models like Calvert [7] Boll [5] and Yung et al [8]. Computational models [9] have also been developed to study the pressure drop and predict the performance of the venturi scrubber.

## 1.2 Problem Statement

Venturi scrubber is one of the most effective pollution control technology for the capturing of the particulates and toxic gases from the contaminated gas streams. It is necessary to have a very deep understanding of the flow physics inside the venturi scrubber for an efficient and economic design.

The focus of present study is to review the pressure drop and dust removal efficiency of forced feed venturi scrubber using CFD simulation. The design parameters like throat gas velocity, loading (L/G ratio) are considered here to predict the optimal performance of venturi scrubber through a model developed in ANSYS FLUENT. Titanium oxide (TiO2) particles having a diameter of 1 micron were taken as dust particles for simulations.

## 1.3 Objectives of Project

The objectives of the present study were:

a) The design of a venturi scrubber computational model in ANSYS FLUENT.
b) To investigate the effect of design parameters on venturi scrubber performance.
c) To find collection efficiency of venturi scrubber having multiple holes at throat under force-feed mode.
d) To validate the simulation results with experimental data.
e) To study the comparison of different flow parameters of venturi scrubber for collection efficiency under the same condition.

## 1.4 Thesis Management

Chapter 1 describes the motivation, problem statement, and objectives of the research. Literature survey related to CFD simulations of venturi scrubber is presented in chapter 2. Chapter 3 explains the models used for simulating turbulence, drag force, particle transport, etc. Chapter 4 describes the geometry formation, meshing and boundary conditions applied to various cases. Chapter 5 presents the results of all cases and their relevant discussions. Chapter 6 depicts the conclusions of this thesis and future recommendations.

# Chapter-2

# Literature Review

This chapter review the preceding work carried out to evaluate the parameters affecting the performance of the venturi scrubber through experimental and computational strategies. The first industrial scale venturi scrubber was installed in 1947 for the removal of salt cake fumes from the Kraft furnace gases [10]. Since then venturi scrubber became paramount in the industry for the abatement of particulate matter. The underlying principle of working of venturi scrubber is the momentum transfer from the incoming high velocity gas stream to the introduced liquid to produce a wide spectrum of droplets. Normally the introduction of liquid either before the throat or in the throat is attained by nozzle bank located in the throat.

Particulate removal in the venturi scrubber is two stage process. The first stage is the contact stage in which the collection is achieved by one of the following collection mechanism depending upon the system requirements.

a) Inertial impaction
b) Interception
c) Brownian diffusion
d) Thermophoresis
e) Diffusiophoresis

The inertial impaction mechanism contributes more than any mechanism to collection process in venturi scrubber [11]. A cyclone separator is installed after venturi scrubber in which the particle laden drops are separated from the clean gas stream. The most reviewed and researched parameters for an efficient and economical design are the pressure drop and collection efficiency. High collection efficiency at low pressure drop has been the most desirable output from any experimental and computational study.

The dispersed multiphase flow inside the venturi scrubber is very complex to understand. The drag force on droplets, liquid disintegration , breakup and coalescence of the droplets, liquid film formation can occur in the venturi scrubber during its operation [9]. Because of the complexities of multiphase flow in venturi scrubber, experimental and numerical interrelationships have been utilized to assess venturi scrubber efficiency. Theoretical models proposed in the literature are based on an understanding of flow physics, design parameters effect on performance estimation and proposed models for pressure drop.

One of the early model proposed by Calvert [4] to predict the pressure drop was based on the assumptions of complete atomization of liquid and achievement of gas velocity by droplets at throat end. It was considered that momentum change of droplets is the main cause of pressure drop in the venturi scrubber neglecting the pressure drop due to gas acceleration and frictional pressure drop. These assumptions result in the following equation:

$$\Delta p = \rho_D \frac{Q_D}{Q_G} U_{GT}^2 \tag{2.1}$$

The equation for pressure drop proposed by Calvert model ignoring the geometric characteristics can result in inadequate predictions.

All the well-known models for performance estimation of venturi scrubber made the assumption of the uniform distribution of droplets and considered the dust is capturing by droplets through inertial impaction. The collection efficiency due to inertial impaction also termed as target efficiency has been derived by Calvert as and linked to Stokes number, as:

$$\eta_t = \left(\frac{St}{St + 0.7}\right)^2 \tag{2.2}$$

The variables which constitute the Stokes number are given as follows:

$$St = \rho_s d_s^2 \frac{|u_i - v_i|}{9\mu d_d} \tag{2.3}$$

With the assumption of a homogeneous distribution of particle of specified diameter and size coupled with gas the flow. Equation 2.4 predicts the number concentration of dust particles as a function of target efficiency. The finite volume method is applied to derive the mass conservation equation for dust particles by Calvert [7] and is given as:

$$-\frac{dn_p}{dx} = \frac{3\,|U_G - U_D| n_p\, H_D}{2 d_D U_G}\,\eta_i \tag{2.4}$$

The droplet motion is described by considering the external drag force, and droplet velocity is calculated by the following derived differential equations:

$$\frac{dU_D}{dx} = \frac{3}{4}\frac{\rho_G}{\rho_D}\,C_D\,\frac{|U_G - U_D|\,(U_G - U_D)}{d_D U_D} \tag{2.5}$$

Boll [5] model presented a differential equation which can be integrated over the venturi . Boll model took into account the gas acceleration, wall friction and droplet acceleration and proposed the following pressure drop equation:

$$-\frac{dp}{dx} = \rho_G\, U_G \frac{dU_G}{dx} + \rho_D \frac{Q_D}{Q_G}\, U_G \frac{dU_D}{dx} + \frac{\left(\frac{Q_D \rho_D}{Q_G \rho_G} + 1\right) \lambda_f \rho_G U_G^2}{2d} \tag{2.6}$$

Hollands and Goel [12] modified the Boll mathematical model . Due to the non-dimensionalized nature of the Boll's equations. General solutions in the form of design charts and equations are obtained for both liquid velocity and pressure drop predictions. Taheri and Sheih [13] presented a model which solves the diffusion equations for both dust and droplets by using particle in cell technique. Placek and Peter[14] came up with

a more realistic model considering the distribution of droplets after a breakup and proposed the following equation for the pressure drop:

$$-\frac{dp}{dx} = \frac{W_G}{A}\frac{dU_G}{dx} + \sum_{i=1}^{n}\frac{W_{D_i}}{A}\ \frac{dU_{D_i}}{dx} + \frac{W_D + W_G}{W_G}\ \lambda_f \frac{1}{2}\frac{\rho_G}{d}\ U_G^2 \tag{2.7}$$

Azzopardi and Govan [6] presented their annular two phase flow model which portray the wall film inside the venturi scrubber. The model considered variation in flow rate of the film because of drag force on film by gas. The model pointed out the existence of a group of droplets at various location along venturi. Pressure drop in the venturi is contributed by frictional pressure drop, accelerational pressure drop and gravity.

Azzopardi and Govan [6] proposed a 1D model for calculating pressure drop and collection efficiency. Liquid flow in the form of a film on the wall was considered, and collection efficiency equation was deduced from the mass conservation for droplets given as:

$$-\left(\frac{dn_p}{dx}\right)_i = \frac{6\eta_i n_p\ |U_G - U_D|\ W_{LE_i}}{\pi d^2 U_G d_{D_i} U_{D_i} \rho_l} \tag{2.8}$$

Viswanathan [15] proposed a model for prediction of pressure drop by considering the droplet and film acceleration as well as wall friction. Model agree well with the experimental data. The pressure recovery in the diffuser section discussed by Azzopardi and Govan model [6] was corrected by Teixeira [16]. Gonclaves et al [3] evaluated the well-known available models for the prediction of pressure drop. The models were compared with experimental data from venturi of different configurations. It was concluded that the model of Azzopardi et al [17] gave satisfactory results for all the variables studied. Sun and Azzopardi [18] extended the boundary layer model [17] known as Full Boundary Layer Model and applied to Pease Anthony type venturi scrubber, and the results agreed well with the experimental results of Yung model [8]. Rahimi et al. [19] model took into account the heat and mass transfer effects in a venturi scrubber. It is concluded that heat and mass transfer results in the reduction of collection

efficiency because of evaporation. Kim et al. [20] presented a comparative study on collection efficiency models available in the literature. The study compared Calvert [7] , Boll [5] and [8] models. Zerwas et al [21] presented CFD simulation of comparison of break up model.

Because of the limitations of the phenomenological models, computational models has been developed and implemented to predict the performance of venturi scrubber. With the recent advancement in computational resources, more sophisticated computational tools are emerged to better resolve the problems better. One such computational tool is Computational Fluid Dynamics (CFD) [22-27].

Ananthanarayanan (1999) utilized the commercial CFD package Fluent to investigate the effect of the nozzle arrangement on liquid flux distribution in a rectangular venturi scrubber. An Eulerian-Lagrangian method was employed to solve the problem. CFD model considers the simple atomization of liquid droplet considering it as the inert particle. The simulation results agree well with the experimental data. The authors suggested improvement of the model in terms of droplet size distribution. Mohebbi et al [28] proposed a model to predict the pressure drop along with the collection efficiency. The developed model strong agreement with experimental data confirmed the Eulerian-Lagrangian method as a powerful tool for performance estimation of venturi scrubber. The model equation for the collection efficiency is as follows:

$$\eta_t = \left(\frac{\Psi_c'}{\Psi_c' + 1}\right)^r \tag{2.9}$$

$$r = 0.759\ \Psi_c'^{-0.245}$$

.

$$\Psi_c' = \rho_s d_s^2 \frac{|u_i - v_i|}{18\mu d_d}$$

To better understand the flow physics inside the venturi scrubber, PAK and CHANG [9] analyzed and studied the dispersed flow numerically inside the venturi scrubber. KIVA code was used as a computational tool. An Eulerian-Lagrangian approach was adopted to solve the model. The model considered the liquid jet atomization, gas and liquid droplets interaction, droplet breakup and collision, droplet deformation because of

aerodynamic forces and dust capture by liquid droplets. The simulated results were validated with experimental data.

Goniva et al. [29] also studied the pressure drop and collection efficiency using a CFD package OPENFOAM. The model considered an Eulerian-Lagrangian scheme for solving the problem. The droplet breakup and coalescence were taken into account. The model also considered the wall film, entrainment of droplets from film and deposition of droplets on wall film. They concluded that the model could be improved by considering accurate droplet size distribution for collection efficiency. Tao [30] studied the role of heat and mass transfer in performance estimation of venturi scrubber. The model was resolved in CFD commercial package ANSYS FLUENT. Droplet dispersion and distribution were studied numerically by Ahmadvand et al. [24]. The CFD model considered the Rosin Rammler distribution of droplets in venturi scrubber and concluded that CFD modeling results agree well with experimental data. They further added that Rosin Rammler distribution parameter $n_{RR}$ depends on the operating parameters like L/G ratio and gas velocity.

Computational modeling and simulation by using commercial CFD package CFX were done by Majid et al. [25, 31] for pressure drop and collection efficiency. The model resolved the turbulence by using k-$\boldsymbol{\varepsilon}$ turbulence model, droplet breakup using CAB model and drag by Schiller-Neumann drag model. The model agreed well with the experimental data [31]. A coupled CFD model with population balance method was developed by Sharifi et al [27]. The Euler-Euler CFD model along with population balance equation to predict the pressure drop was used. They concluded that for the pressure drop is independent of different configurations and diameters of nozzles.

In the present model, the dispersed three phase flow is numerically investigated. The aim of the present study is two-fold, firstly the investigation of the effect of design variables like throat velocity, L/G ratio effect on performance parameters. Secondly the simulation outcomes validation with the experimental data [32]. Moreover, the simulated results obtained for collection efficiency by using equation (12) and equation (14) are to be compared for best fit with the experimental data.

# Chapter-3

# Mathematical Modeling

CFD is a very powerful tool to be used for simulation of any real and physical system to understand its working before going to perform experiments. Certain models are used in CFD to understand the flow physics by utilizing a set of equations. The numerical methods are used to solve these equations.

## 3.1 Assumptions for Model development:

A mathematical model which describes the physical phenomena occurring inside the venturi scrubber can be developed by making following assumptions:

a) Gas is incompressible, Newtonian fluid.
b) Unidirectional flow of droplet and gas.
c) Dust loading is very low and has a negligible effect on the gas phase.
d) Droplets are assumed to be a sphere.
e) Droplets are uniformly distributed along the venturi throat.
f) Negligible heat and mass transfer between phases during flow.

## 3.2 Multiphase Flow Modeling:

The dispersed three phase flow involving gas, dust (solid) and a droplet (liquid) is the multiphase flow in venturi scrubber. A simple multiphase flow is defined as “the flow in which different phases are involved.” [33].

### 3.2.1 Multiphase flow regimes

Flow regimes refer to the flow pattern that arises during flow depending upon flow rates and materials also. Flow regimes that encountered during flow are shown schematically in Figure 3.1:

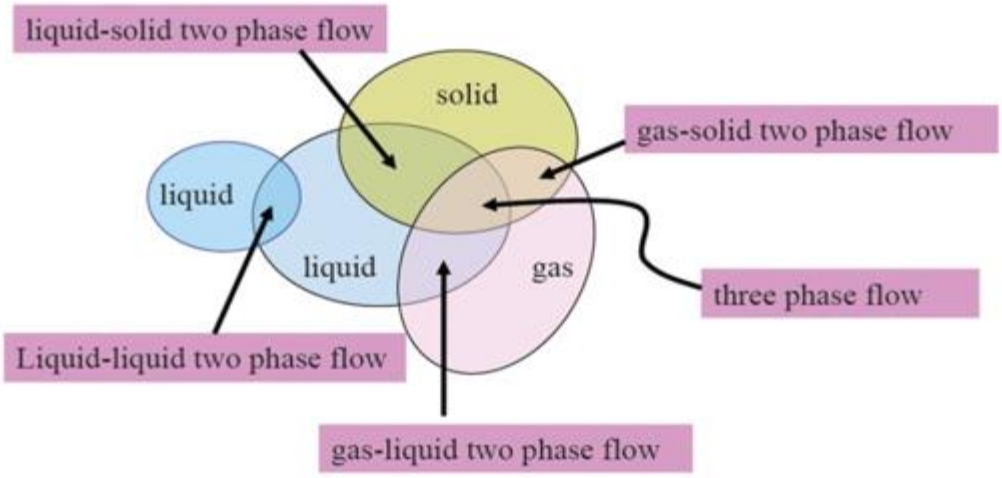


**Figure 3.1 Multiphase flow regime [34]**

### 3.2.2 Basic terminologies of multiphase flow

The terminologies encountered in the multiphase flow are discussed in this section. The term discrete refers to the particles while continuously refers to the carrier fluid.[33].

#### 3.2.2.1 Dispersed phase flow

The flow which comprises of discrete elements like dust particles is known as dispersed phase flow. The discrete elements are not connected.

#### 3.2.2.2 Volume fractions and density

Volume fraction of discrete phase is given as:

$$\alpha_d = \lim_{\delta V \to V^0} \frac{\delta V_d}{\delta V} \tag{3.1}$$

The volume fraction of the continuous phase is

$$\alpha_c = \lim_{\delta V \to V^0} \frac{\delta V_c}{\delta V} \tag{3.2}$$

By definition, the sum of the volume fraction of dispersed and continuous phase must be unity:

$$\alpha_d + \boldsymbol{\alpha_c} = \mathbf{1} \tag{3.3}$$

The bulk density (or apparent density) of the dispersed phase is given as:

$$\overline{\rho_d} = \frac{\lim_{\delta V \to V^0} \delta M_d}{\delta V} \tag{3.4}$$

The sum of bulk densities of dispersed and continuous phase is given as:

$$\overline{\rho_d} + \overline{\rho_c} = \boldsymbol{\rho_m} \tag{3.5}$$

### 3.2.2.3 Superficial and phase velocity

Superficial velocity in multiphase flow is the velocity attains by the fluid in any close channel in the absence of packing as given below.

$$\mathrm{U_d} = \frac{\dot{\mathrm{M}}_\mathrm{d}}{\rho_\mathrm{d} \mathrm{A}} \tag{3.6}$$

The phase velocity is the actual velocity that a fluid attain during flow. Superficial and actual velocity are related as

$$\mathrm{U_d} = \alpha_\mathrm{d}\, \mathrm{u_d} \tag{3.7}$$

### 3.2.2.4 Quality, Concentration and Loading

Concentration [35] is the common term in multiphase flow. It is the mass ratio of dispersed phase mass to continuous phase mass as given below:

$$\mathrm{C} = \frac{\overline{\rho_\mathrm{d}}}{\overline{\rho_\mathrm{c}}} \tag{3.8}$$

The term quality refers to the liquid in the dispersed phase and is given as:

$$\mathrm{x} = \frac{\overline{\rho_\mathrm{d}}}{\overline{\rho_\mathrm{m}}} \tag{3.9}$$

Loading, which is the ratio of mass flux of the dispersed phase to that of the continuous phase is given as:

$$z = \frac{\dot{m}_d}{\dot{m}_c} \tag{3.10}$$

For modeling multiphase flow in CFD, there are two approaches that are generally utilized to address the multiphase flow problem.

I. Eulerian-Eulerian approach

II. Eulerian-Lagrangian approach

### 3.3 Eulerian-Eulerian approach

Models treated by Eulerian-Eulerian approach are commonly known as multi-fluid models. In the Eulerian-Eulerian approach, the phases are treated as the interpenetrating continua. Dispersed phase can also be treated in the Eulerian frame of reference. Dense flows can be treated in the Eulerian frame of reference as there loading is high. The conservation equations are solved for phase separately. Along with the transport equations, the equations for the volume fraction of each phase is also solved. Governing equation for Eulerian approach is given as[36].

$$\frac{\partial \alpha_k \rho_k}{\partial t} + \nabla . (\alpha_k \rho_k U_k) \tag{3.11}$$

$$\frac{\partial \alpha_k \rho_k U_k}{\partial t} + \nabla . (\alpha_k \rho_k U_k U_k) = -\alpha_k \nabla P + \alpha_k \nabla . \tau_k + \alpha_k \rho_k g_k + S_k = 0 \tag{3.12}$$

$$\frac{\partial \alpha_k}{\partial t} + \nabla . (\alpha_k U_k) = 0 \tag{3.13}$$

U refers to the mean velocity field and P is the mean pressure shared by the phases. The subscript k refers to the $k_{th}$ continuous phase.

In ANSYS Fluent the Euler-Euler approach is utilized by the following three models [36]:

a) The volume of fluid (VOF) model.

b) The mixture model.

c) The Eulerian model.

### 3.3.1 The volume of fluid (VOF) model:

The volume of fluid method is an interface tracking method. A single set of momentum equation is shared by both the fluids. Indicator function also known as the color function represents the volume fraction of each phase. An indicator function having a value of 1 represents the presence of one phase in a cell while the value between 0 and 1 refers to the interface between the phases in a control volume.

Further details can be found elsewhere [33, 35, 36].

### 3.3.2 The Mixture model:

The mixture model can treat two or more phases (fluid or particulates) as interpenetrating continua. The mixture model solves the momentum equation for the mixture and relative velocities are utilized to describe the dispersed phases. Details can be found elsewhere [33, 35, 36] .

### 3.3.3 The Eulerian model:

The Eulerian model is the most complex multiphase model. It solves a set of momentum and continuity equation for each phase. Coupling between the phases is achieved through the interphase exchange coefficients. Secondary phases can be treated in Eulerian phase also. Drag between the phases can also be modeled by the build in drag laws in the Eulerian model. Details of the Eulerian model can be found elsewhere [33, 35, 36].

## 3.4 Eulerian-Lagrangian approach

In the Euler-Lagrange approach, carrier or continuous phase is treated in Eulerian framework while the particles are tracked in the Lagrangian framework. Particle here refers to the solid particle or gas/ fluid bubble/droplet. Conservation equations are solved for the continuous phase while the equation of motion is applied to particles in the computational domain.

### 3.4.1 Continuous phase modeling

#### 3.4.1.1 Continuity Equation:

The continuous phase is treated in the Eulerian framework. The continuity equation is given as:

$$\frac{\partial \rho}{\partial t} + \nabla . (\rho \overrightarrow{v}) = S_{DPM} + S_{other} \tag{3.14}$$

### 3.4.1.2 Momentum equation:

Momentum equation can be considered as an alternative form of Navier Stokes equations. These equations are derived on the basis of Newton's motion law. The time rate of change of momentum is equal to the sum of all the forces experienced by the fluid element. These forces may include body forces, surface and pressure forces. The momentum equation is given as:

$$\frac{\partial \rho \overrightarrow{v}}{\partial t} + . (\rho \overrightarrow{v} \overrightarrow{v}) = -\nabla p + \nabla . \tau + \rho \overrightarrow{g} + \overrightarrow{F}_{DPM} + \overrightarrow{F}_{other} \tag{3.15}$$

### 3.4.2 Dispersed phase modeling:

Dust and droplets are tracked in the Lagrangian frame of reference as Lagrangian framework rigorously modeled the particle level phenomena for dispersed phase flow. Particles to be tracked are introduced in the computational domain as a parcel. A computational parcel contains a specific number, size, location and temperature of particles contained within it. The integration of the force balance upon particle yields the trajectory of the particle in the computational domain. The force balance is given as:

$$\frac{du_i^p}{dt} = \overbrace{F_D \left(u_i - u_i^p\right)}^{\text{Drag force}} + \overbrace{g_i \frac{\rho_p - \rho}{\rho_p}}^{\text{Gravity force}} + \overbrace{\frac{\overrightarrow{F_i}}{\rho_p}}^{\text{Additional forces}} \tag{3.16}$$

### 3.4.3 Interphase transfer through source terms:

In the Lagrangian framework, particle trajectory is calculated. As the continuous phase always impacts the discrete phase, this is known as one way coupling. Similarly, the particle can also affect the continuous phase which is two way coupling. This coupling can be achieved through the mass, momentum and energy equations [36]. The qualitative description of the two way coupling is depicted in Figure 3.2.

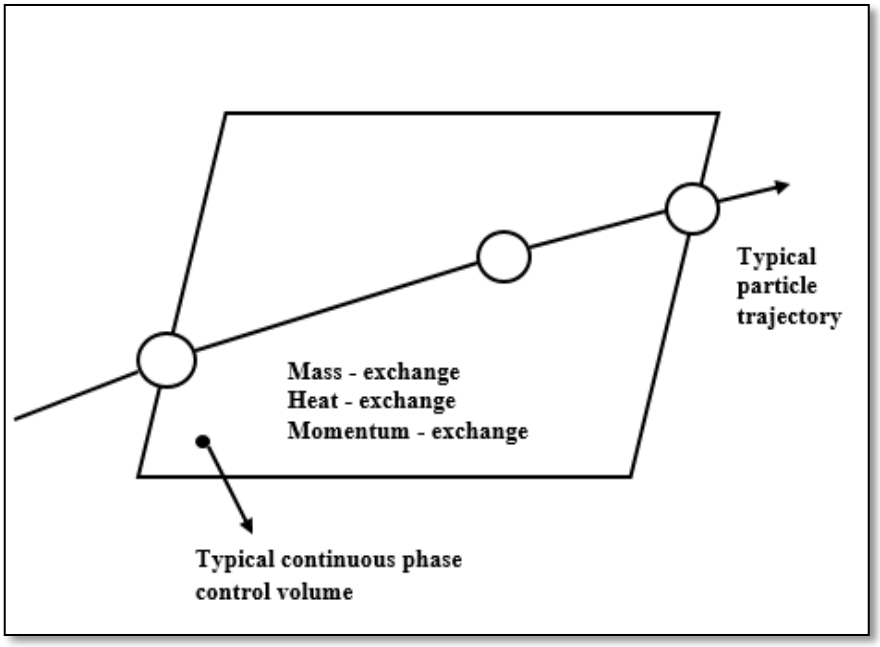


**Figure3-2 Heat, Mass and Momentum transfer between the Discrete and Continuous phase [36]**

## 3.5 Turbulence Modeling:

The turbulence of the present system is modeled through the realizable k-**ε** turbulence model.. The realizable k-**ε** model differs from other k-**ε** models in two different ways [36]:

a) Realizable k- **ε** model contains an alternative formulation for turbulent viscosity.

b) A modified equation for dissipation rate **ε** is also incorporated.

The modeled transport equations for k and **ε** in the realizable k-ϵ model are:

$$\frac{\partial}{\partial t}(\rho k) + \frac{\partial}{\partial x_j}\left(\rho k u_j\right) = \frac{\partial}{\partial x_j}\left[\left(\mu + \frac{\mu_t}{\sigma_k}\right)\frac{\partial k}{\partial x_j}\right] + G_k + G_b - \rho\varepsilon - Y_M + S_k \tag{3.17}$$

$$\frac{\partial}{\partial t}(\rho\varepsilon) + \frac{\partial}{\partial x_j}\left(\rho\varepsilon u_j\right) = \frac{\partial}{\partial x_j}\left[\left(\mu + \frac{\mu_t}{\sigma_\varepsilon}\right)\frac{\partial \varepsilon}{\partial x_j}\right] + \rho C_1 S_\varepsilon - \rho C_2 \frac{\varepsilon^2}{k + \sqrt{v\epsilon}} + C_{1\epsilon}\frac{\epsilon}{k}\, C_{3\varepsilon}\, G_b + S\epsilon \tag{3.18}$$

Generation of turbulent kinetic energy due to mean velocity gradients and buoyancy is predicted by equation 3.18. $Y_M$ represents the dilatation dissipation term, $C_2$ and $C_{1E}$ are constants $\boldsymbol{\sigma}_k$ and $\boldsymbol{\sigma}_{\boldsymbol{\varepsilon}}$ are the turbulent Prandtl numbers.

### 3.6 Droplet Breakup modeling:

Droplet formation happened when the aerodynamic forces and turbulence of gas causes a droplet to deform and breakup into child droplets. The droplet breakup criterion is computed with the standard TAB model. TAB model is established upon the analogy between an oscillating and distorting droplet and spring mass system. The equation describing the damping force oscillator is given as:

$$\frac{md^2x}{dt^2} + b\frac{dx}{dt} + cx = F \tag{3.19}$$

Where F is the aerodynamic force, the restoring force cx is given by the surface tension whereas the damping term $b\frac{dx}{dt}$ is due to liquid viscosity. Droplet breakup will occur when $x > \frac{r}{2}$ where $x$ is the displacement of the droplet equator from its spherical (undisturbed) position. The droplet distortion is described as:

$$\frac{d^2y}{dt^2} = \frac{C_F\rho_g u^2}{C_b\rho_l r^2} - \frac{C_k\sigma}{\rho_l r^3}y - \frac{C_d\mu_l}{\rho_l r^2}\frac{dy}{dt} \tag{3.20}$$

Y represents the droplet distortion. Weber number represents the characteristic breakup of the droplet as it is the ratio of aerodynamic forces to that of surface tension forces.

$$We = \frac{\boldsymbol{\rho_g u^2 r}}{\sigma} \tag{3.21}$$

The high Weber number will represent the droplet deformation, and the aerodynamic forces on the droplet will be dominant as compared to that of that of the surface tension of the droplet. Droplet distortion is qualitatively presented in Figure 3.3.

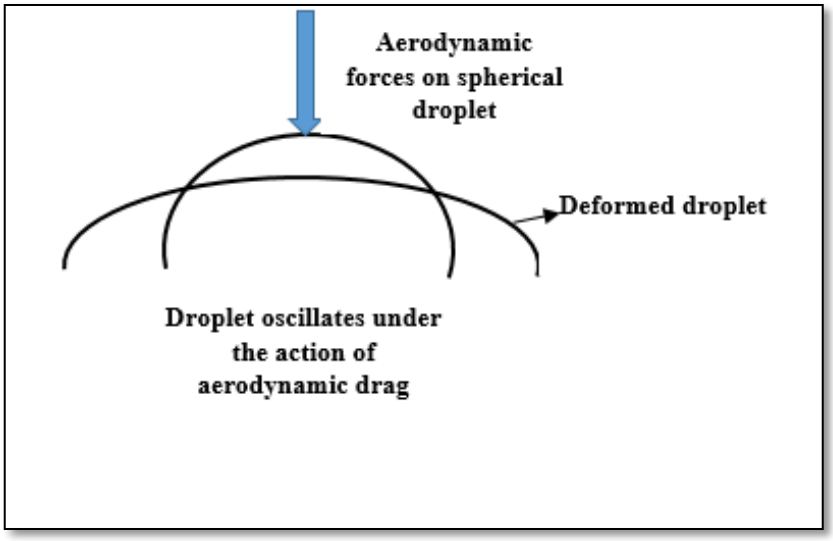


**Figure 3-3 Oscillating droplet under the action of aerodynamic drag [29]**

The oscillations will grow to a critical value, and the parent droplet will break into child droplets. The size and velocity of the child droplets can be evaluated from the energy balance [36, 37].

## 3.7 Drag coefficient modeling:

### 3.7.1 Spherical drag law for dust particles:

For modeling the drag- coefficient for dust particles and liquid droplets dedicated drag model are used. For dust particles as they are spherical, spherical drag law is used for the drag coefficient. From the Morsi and Alexander model [38].

$$f = \frac{C_D R_e}{24} \tag{3.22}$$

$$C_D = a_1 + \frac{a_2}{R_e} + \frac{a_3}{R_e^2}$$

Where $a_1$, $a_2$ and $a_3$ are the constants given by Morsi and Alexander for different Re.

#### 3.7.2 Dynamic drag law for droplets:

The droplet deforms and ultimately breakup under the action of aerodynamic forces. The drag on the droplet during deformation changes as the shape of the droplet is distorted.

The drag on a deforming droplet is modeled with the dynamic drag law which takes into account the deformation of the droplet. The drag coefficient is given by:

$$C_d = C_{d,sphere}\ (1 + 2.632y) \tag{3.23}$$

Where $C_{d,sphere}$ shows the drag for the spherical droplet and given as:

$$C_{d,sphere} = \begin{cases} 0.424, & R_e > 1000 \\ \dfrac{24}{R_e\left(1 + \frac{1}{6}R_e^{0.666}\right)}, & R_e \leq 1000 \end{cases}$$

### 3.8 Modeling of dust capture:

The dust particles are collected in a venturi scrubber by droplets. The collection mechanism depends upon the size of the dust particles. Depending upon the diameter of dust particles, different mechanisms can enhance the effectiveness of scrubber which are as follows**:**

a) Interception
b) Inertial impaction
c) Brownian diffusion

#### 3.8.1 Interception:

The interception collection mechanism will be effective only if the dust particles are in the vicinity of the droplets. The particles will be collected by the droplet due to interception, if the streamlines of gas flow carrying the dust particles are within the range of one particle diameter. The mechanism of the interception is shown in Figure 3.4:

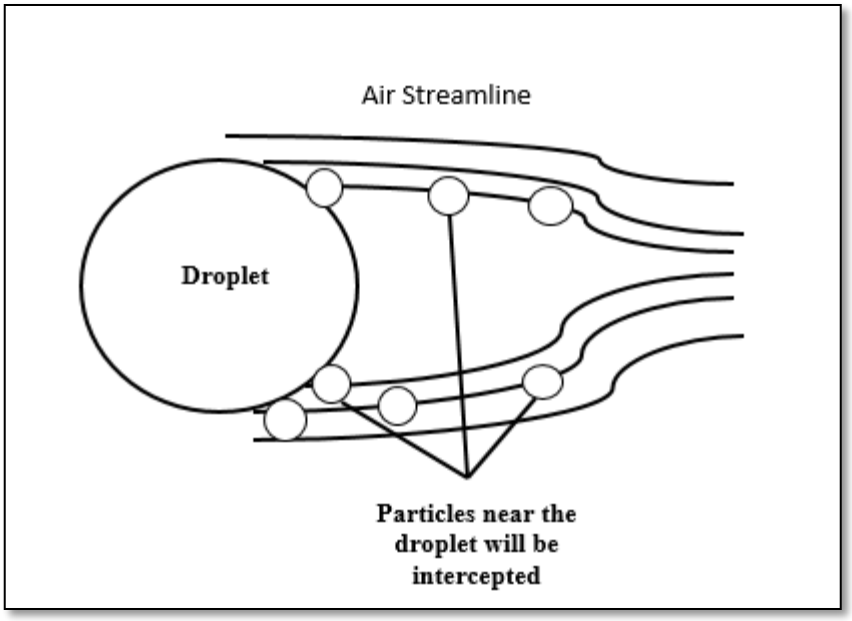


**Figure 3-4 Interception phenomenon [33]**

### 3.8.2 Inertial Impaction:

Dust particles move with the gas phase velocity in the venturi scrubber. The dust particles trajectory is governed by two forces acting on it. The drag force by the gas and its inertia itself. When the dust particles reach the droplet, due to its inertia, it impact on the droplet and hence collected and captured by the droplet as shown in Figure 3.5. This is known as inertial impaction and is the major collection mechanism in the venturi scrubber [20].

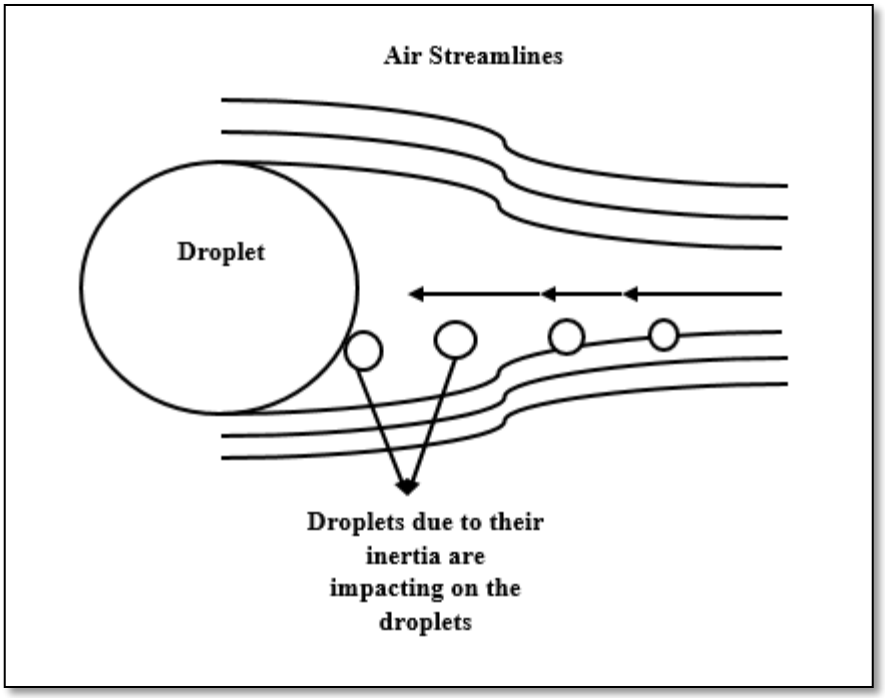


**Figure 3-5 Inertial Impaction [33]**

### 3.8.3 Brownian diffusion:

Dust particle removal by diffusion takes place due to both motion of the particle and the Brownian motion. The particle motion causes a direct particle-liquid interaction, which results in removal of particle only. This phenomenon is significant for particles having a size less than 0.1 μm in diameter.

Brownian diffusion is dominant for low air velocities and smaller particles diameter as shown in Figure 3.6. Since diffusion is always a slow process so, low velocity helps in providing more time for the mechanism to take place.

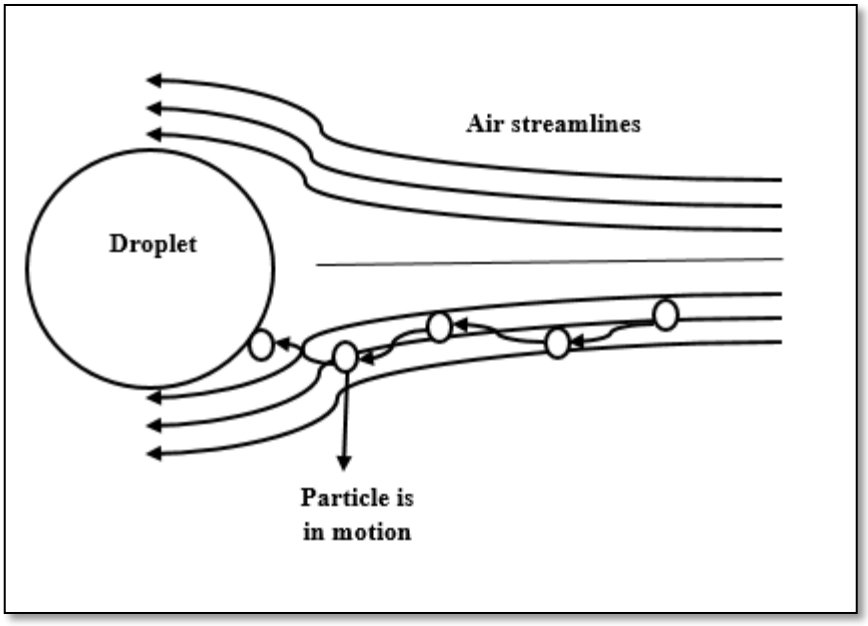


**Figure 3-6 Brownian diffusion [33]**

### 3.8.4 Target efficiency

The dust particle that is simulated in the present research is of 1 μm diameter so the dominant collection mechanism is inertial impaction. The target efficiency which is the impaction efficiency is given as [7] :

$$\eta_t = \left(\frac{\Psi_c}{\Psi_c + 0.7}\right)^2 \tag{3.24}$$

Here $\Psi_c$ is defined as the inertial impaction parameter/ Stokes number and given as

$$\Psi_c = \rho_s d_s^2 \frac{|u_i - v_i|}{9\mu d_d}$$

Another target efficiency equation reported by Mohebbi et al [28] is given as:

$$\eta_t = \left(\frac{\Psi_c'}{\Psi_c' + 1}\right)^r \tag{3.25}$$

$$r = 0.759\ \Psi_c'^{-0.245}$$

$$\Psi_c' = \rho_s d_s^2 \frac{|u_i - v_i|}{18\mu d_d}$$

The present research utilizes both the target efficiency to compare the simulated results obtained from both the equations.

# Chapter-4

# Numerical Methodology

The present work focuses on the venturi scrubber performance improvement in terms of collection efficiency and pressure drop. The venturi scrubber under consideration is the Pease-Anthony forced feed venturi scrubber.

The numerical methodology involves the following:

a) Geometry creation
b) Boundary Conditions
c) Solver Setting
d) Post Processing.

## 4.1 Geometry Creation

The venturi scrubber model is developed in the Design Modeler. The dimension of the model is taken from the previous work [29]. The front and isometric view of the venturi scrubber model prepared in Design Modeler is given in Figure 4.1. The dimensions of the venturi scrubber model are summarized in Table 4.1.

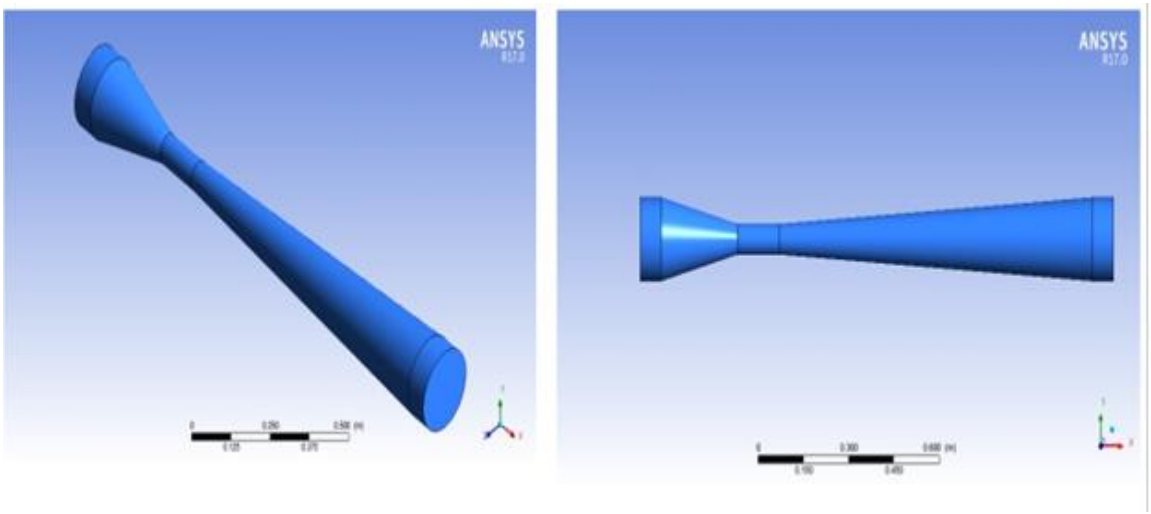


**Figure 4-1 Venturi Scrubber Geometry isometric and front view**

**Table 4-1 Dimensions for Venturi scrubber model**

| Characteristics | Dimensions (meter) |
|---|---|
| Inlet Cylinder length | 0.07 |
| Converging section length | 0.252 |
| Throat length | 0.140 |
| Throat diameter | 0.07 |
| Diverging section length | 1.037 |
| Inlet & Outlet Diameter | 0.192 |
| No of orifices | 12 |
| Exit Cylinder length | 0.07 |

#### 4.1.1 3-D geometry creation in Design Modeler

The three-dimensional geometry is created in Design Modeler. Firstly, sketches are made on the respective planes according to the dimensions and then revolve command is applied to create the venturi scrubber geometry that is also a computational domain as depicted in Figure 4.2.

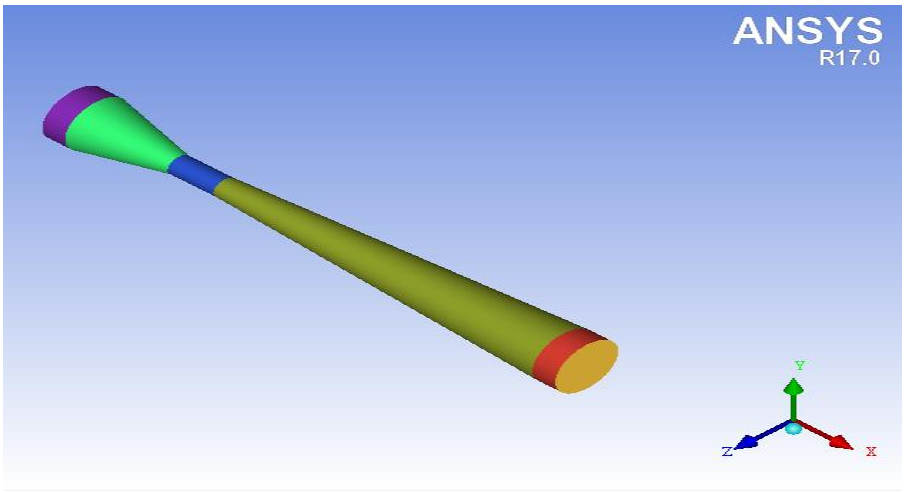


**Figure 4-2 Venturi scrubber computational domain**

## 4.2 Meshing

When doing simulations in ANSYS, the solution of the problem depends strongly on the mesh quality. It is very necessary to have a reasonable mesh to solve the problem. The meshing of the computational domain is done in ANSYS ICEM CFD. ANSYS ICEM CFD is a sophisticated tool for mesh creation.

The overall process of mesh generation is highlighted in Figure 4.3 below:

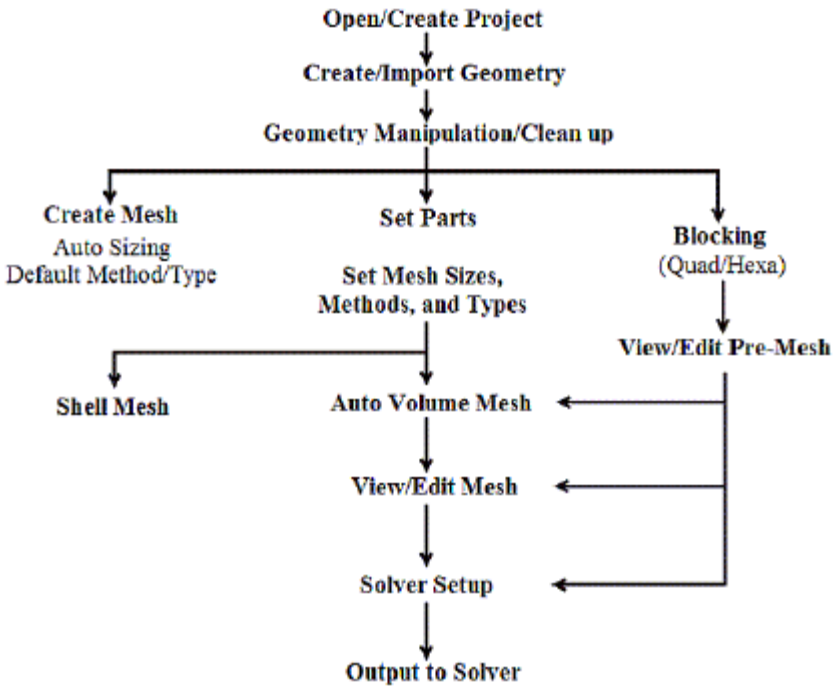


**Figure 4-3 Overall process of mesh generation [22]**

### 4.2.1 Steps of Creating Mesh

Following steps are performed for the mesh creation:

a) Geometry import to ICEM CFD.

b) Blocking of the geometry.

c) Splitting of the Blocks according to the requirement.

d) Blocking associations are done.

e) The setting of the edge parameters.

f) Generating Pre-mesh.

g) Checking quality.

h) Setting output solver.

The blocking of the venturi scrubber computational domain is depicted in Figure 4.4.

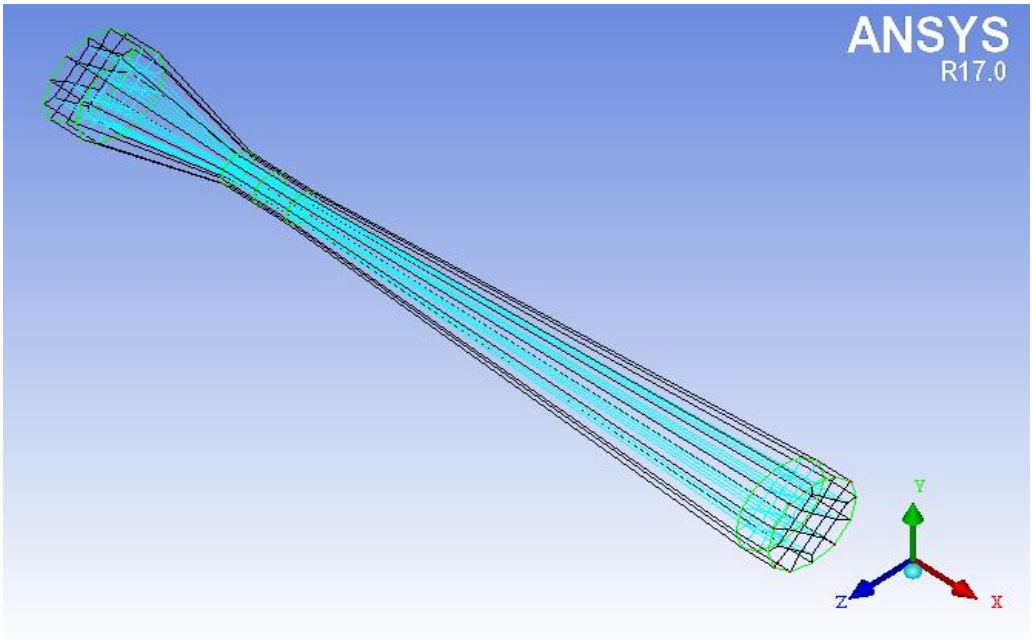


**Figure 4-4 Blocked Geometry of venturi scrubber**

The unstructured HEXA mesh is generated in ICEM CFD and is shown in Figure 4.5 and Figure 4.6.

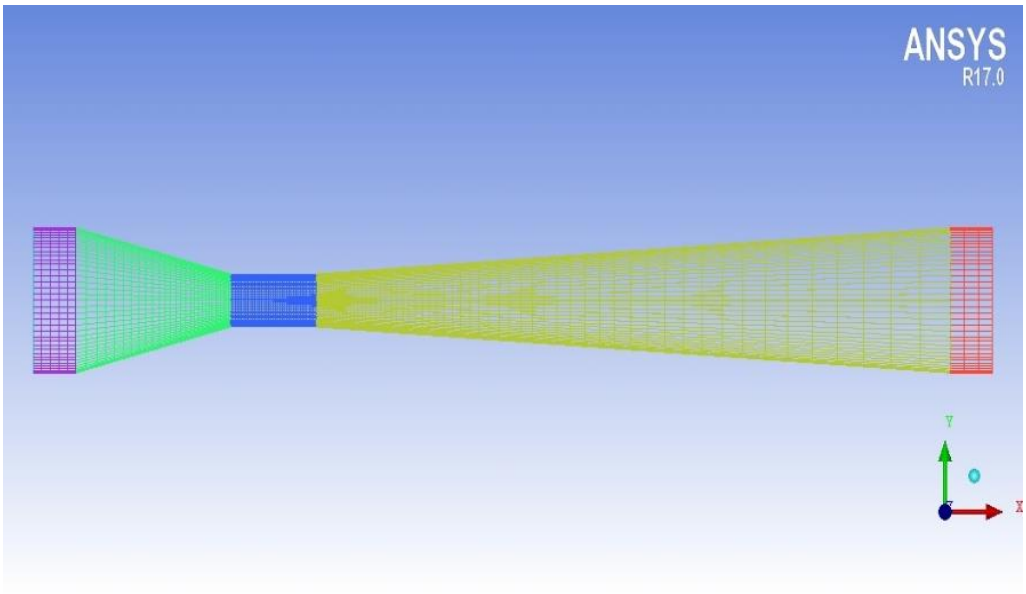


**Figure 4-5 Front view of the mesh of venturi scrubber**

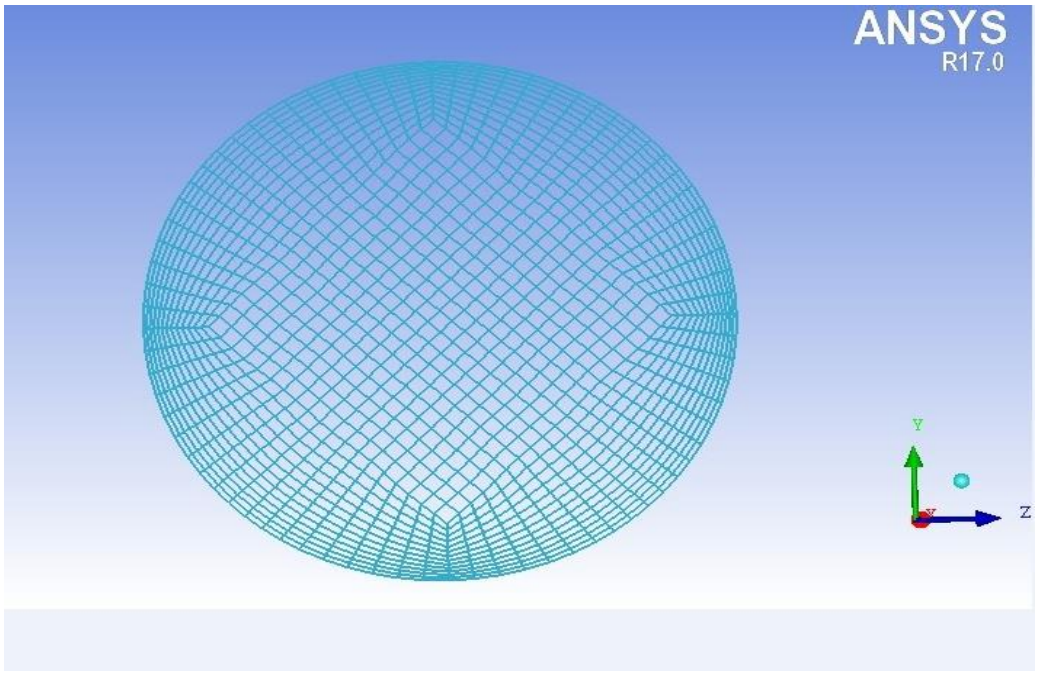


**Figure 4-6 Mesh at inlet of venturi scrubber**

The quality of the mesh created for the present model is above 0.6 which is in accordance with the mesh quality criteria defined by ICEM CFD.

### 4.2.2 Mesh Independency:

In CFD analyses of any problem, the results of the problem are highly dependent on the mesh size and elements. The aim of mesh independence study is to check at what number of elements the solution becomes independent from the element size. Three different meshes are created whose details are given in Table 4.2.

**Table4-2 Details of meshes for mesh independence**

| Mesh | No. of Elements |
|---|---|
| Coarse mesh | 109846 |
| Medium mesh | 194240 |
| Fine mesh | 413853 |

Graph between the distance along the venturi and velocity shows that the mesh becomes independent at 413853 elements. The result is shown in Figure 4.7.

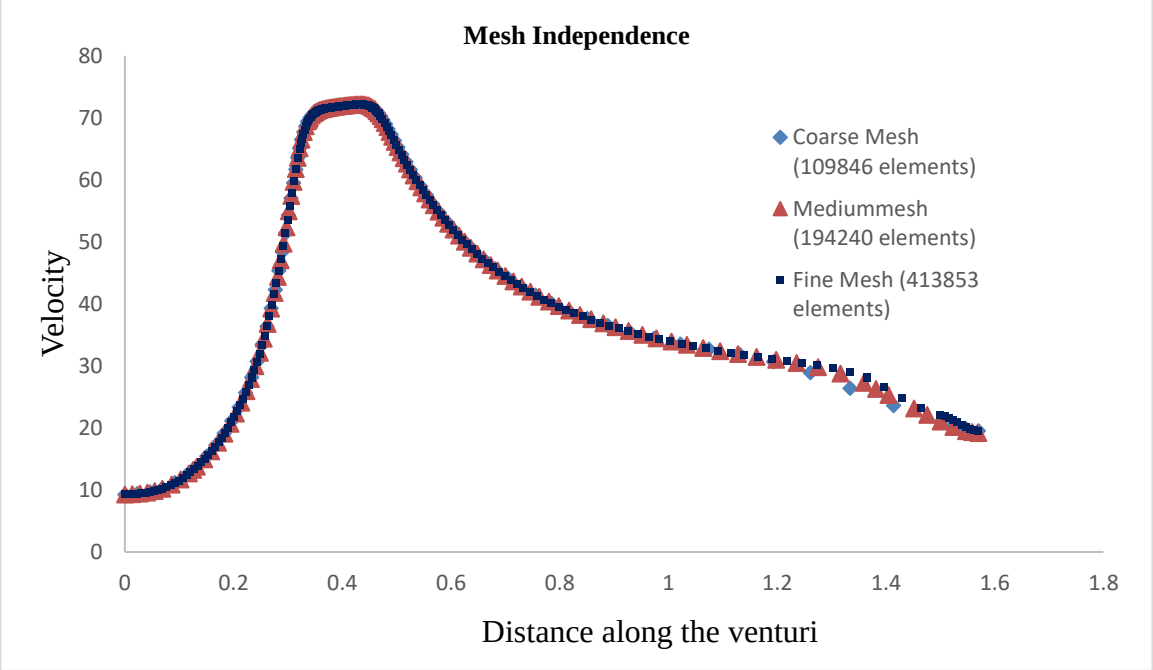


**Figure 4-7 Mesh independence (Velocity)**

## 4.3 Boundary condition

Boundary conditions specify the flow and thermal variables on the boundaries of the physical model. Boundary condition should be specified according to the conditions, as they are a critical component of ANSYS FLUENT simulations [36].

### 4.3.1 Available Boundary types in ANSYS FLUENT

Boundary types in ANSYS FLUENT are of the following three types:

a) Flow boundaries.
b) Wall, repeating and pole boundaries.
c) Internal face boundaries.

The boundary conditions for the present model are the flow inlet and exit boundaries along with wall boundaries as depicted in Figure 4.8 and are given as:

i. Gas Entry: Prescribed as velocity inlet for gas, while dust particles are injected as group injection with a mean diameter of 1 μm.

ii. The exit of Gas and Liquid: Marked as pressure outlet.

iii. Liquid Injection: Liquid is injected from the plain orifice atomizer injection type with a mass flow rate boundary condition.

iv. Equipment walls: No slip boundary condition is prescribed at the walls.

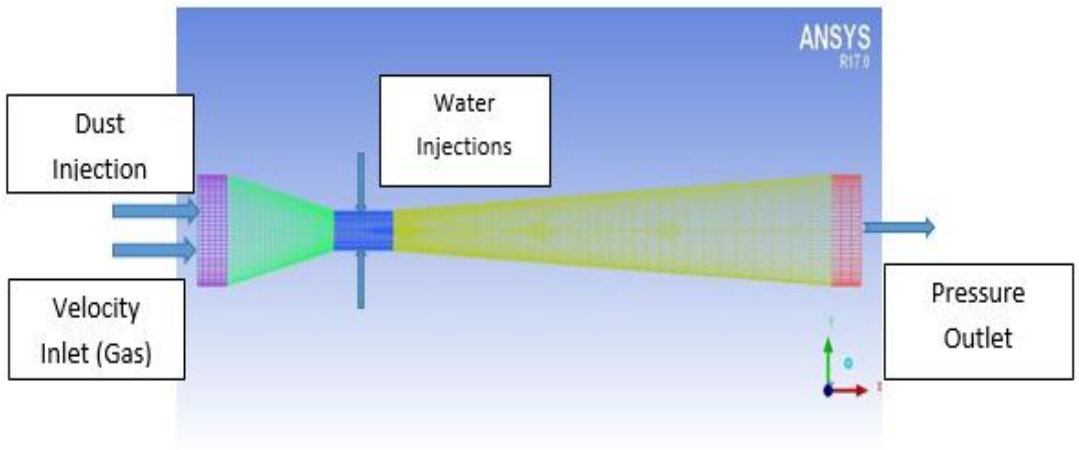


**Figure 4-8 Boundary conditions**

## 4.4 Convergence criteria:

The standard convergence criterion of $10^{-3}$ of the ANSYS FLUENT is defined for all the residuals.

# Chapter-5

# Results and Discussion

The objective of the present work was to find the performance estimation parameters and the investigation of the design parameters on the performance parameters. The performance parameters like collection efficiency and pressure drop are evaluated at different throat velocities and different liquid to gas (L/G) ratios.

## 5.1 Pressure drop

Pressure drop is the most important performance parameter that determines the energy costs of the venturi scrubber. When the gas flow through the venturi scrubber it is accompanied by a pressure drop which can be a combination of different pressure drops. In the case of venturi scrubber, these pressure drops are as under:

a) Frictional pressure drop
b) Acceleration pressure drop (gas)
c) Acceleration pressure drop (droplets)
d) Acceleration pressure drop (film)
e) Gravitational (static) pressure drop

### 5.1.1 Single phase pressure drop (Effect of throat gas velocity on pressure drop)

It can be observed from the graph in Figure 5.1 that as the gas velocity increase the pressure drop in the venturi scrubber increases. Gas accelerates in the convergent area results in the pressure drop according to the Bernoulli's equation.

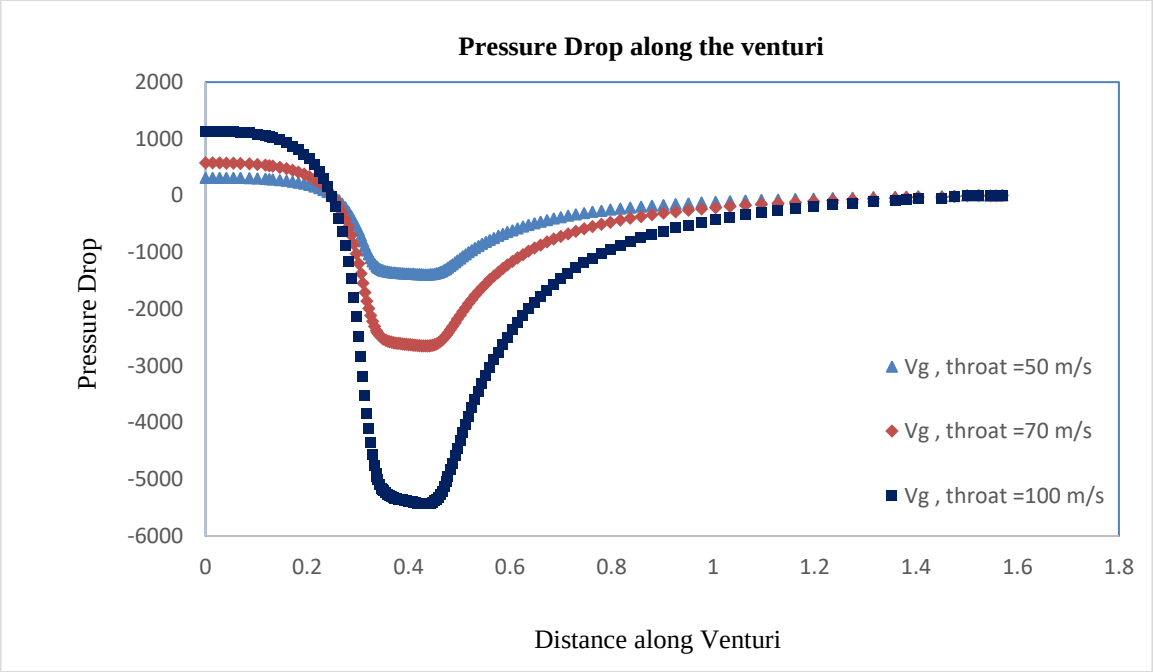


**Figure 5-1 Single phase pressure drop at different throat velocities.**

### 5.1.2 Effect of L/G ratio on pressure drop

Liquid injection mode is used for the introduction of liquid as a spray in venturi scrubber throat. As the liquid is injected in the throat section, the pressure drop increases as shown in Figure 5.2.

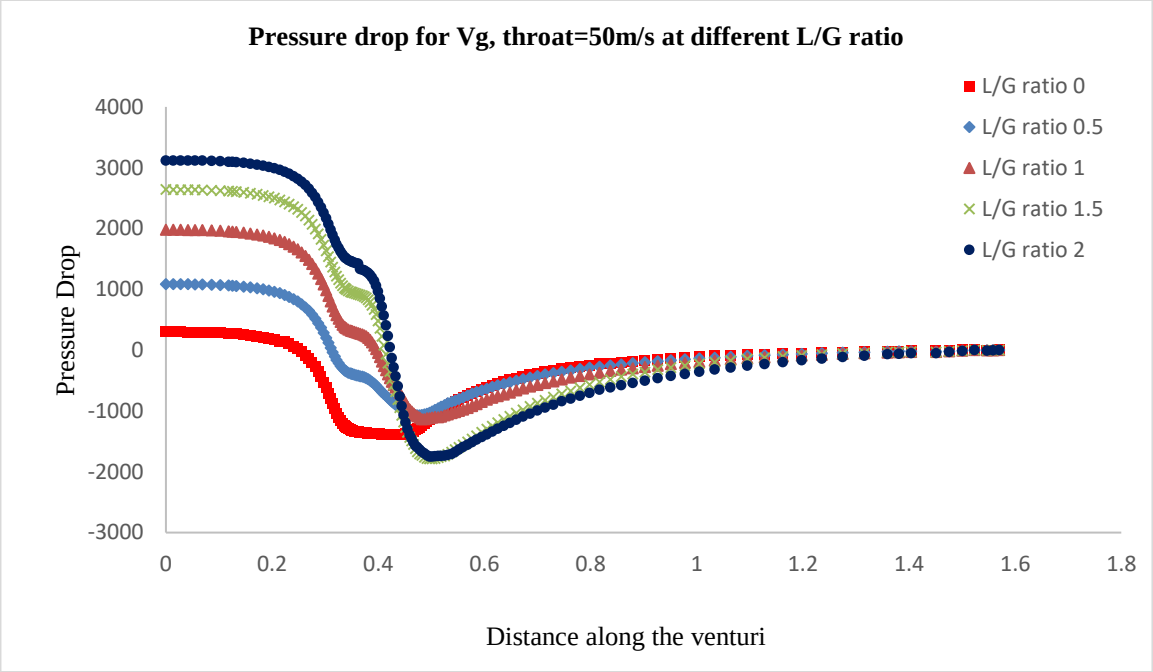


**Figure 5-2 Pressure drop variation for Vg, throat =50 m/s at different L/G ratio**

Pressure drop dynamically increased after liquid introduction. The increase in L/G ratio depicts the increase of the liquid flow rate. The increase in the liquid flow rate also increases the penetration of the spray transversally in the throat section. The pressure drop dynamic increase after the introduction of the second liquid phase refers to the contribution of the acceleration pressure drop (droplets) to the frictional pressure drop and acceleration pressure drop (gas).

The result also satisfies the theory behind the venturi scrubber that the gas kinetic energy gained by the gas in the converging section is utilized in droplet disintegration and also in accelerating them. This behavior can be seen in Figure 5.3. The contours of the pressure drop for a throat gas velocity of 50 m/s at different L/G ratio clearly indicates the when the liquid proportion increases in the throat section, the pressure dynamically reduced. This is due to the reason that gas momentum is utilized in droplet breakup and acceleration as mentioned above.

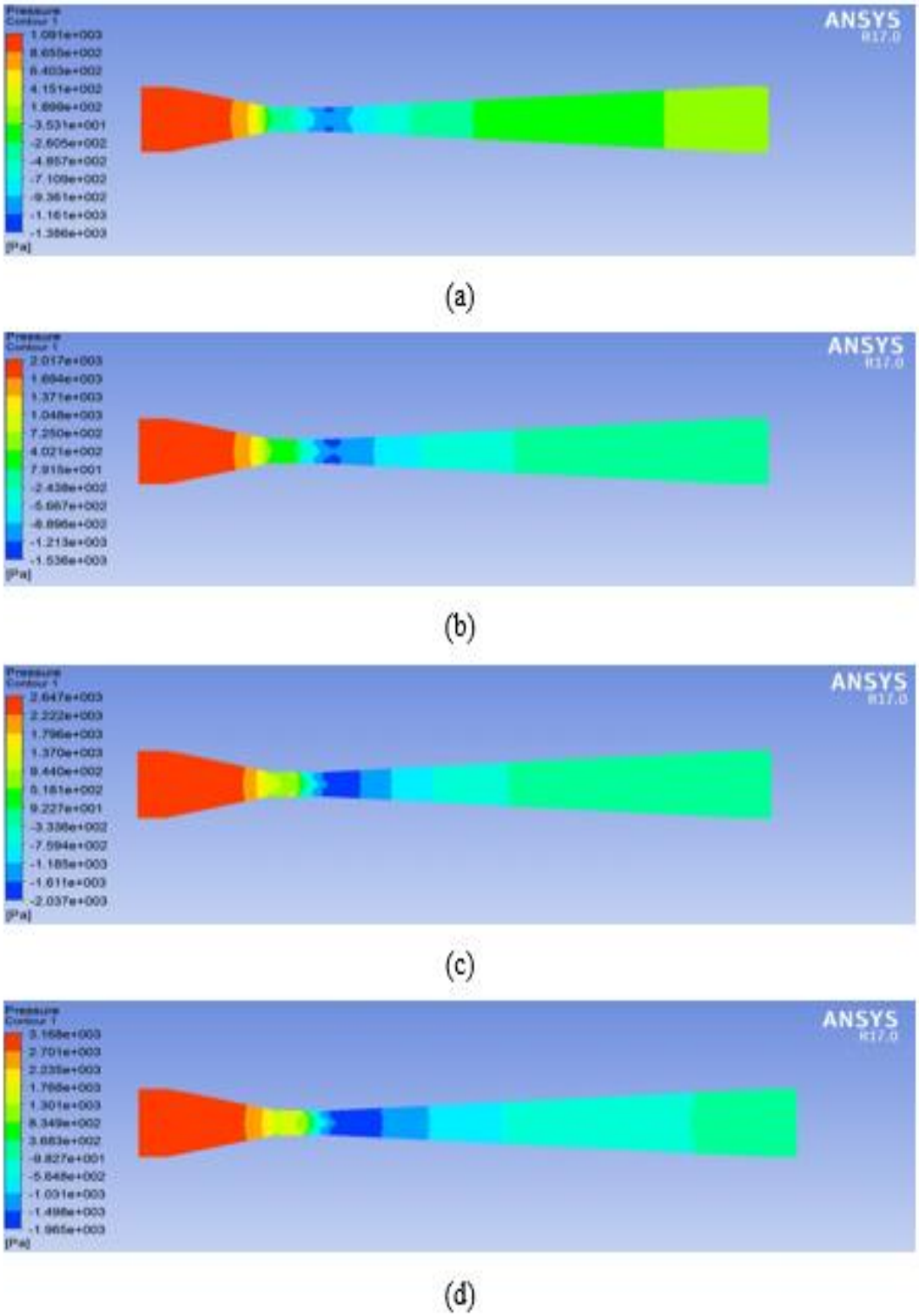


**Figure 5-3 Pressure Drop contours for Vg, throat=50 a) L/G ratio=0.5, b) L/G ratio=1 c) L/G ratio=1.5, d) L/G ratio=2**

As the liquid flow rate increases, the pressure drop increases as depicted in Figure 5.4.

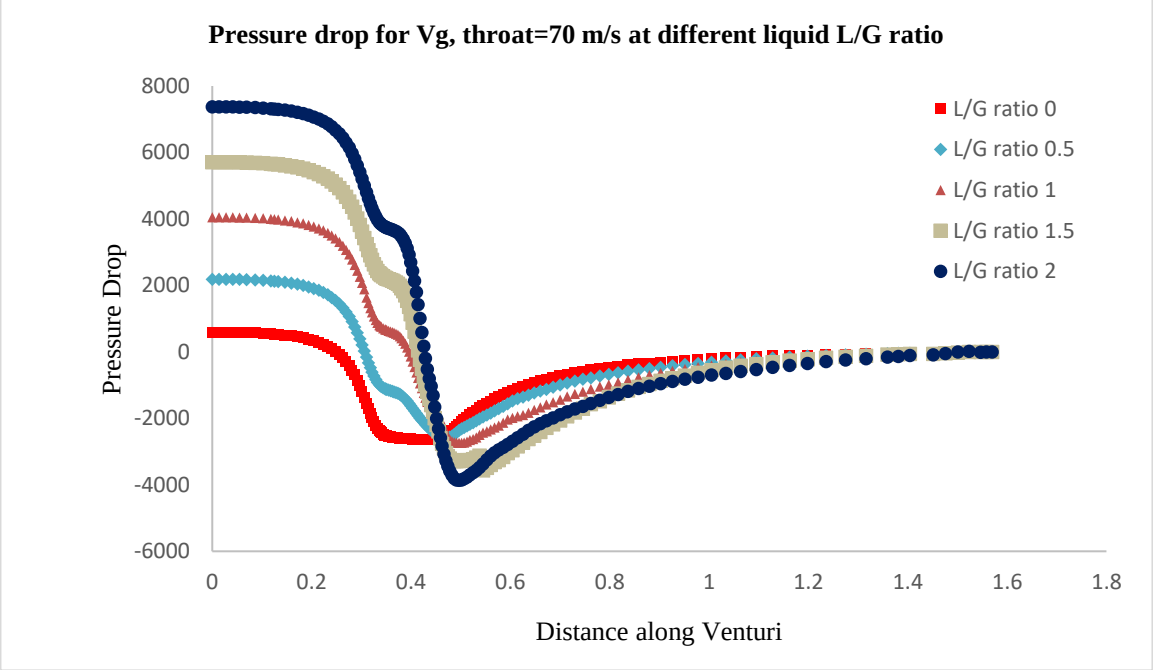


**Figure 5-4 Pressure drop for Vg, throat=70 m/s at different L/G ratio**

The simulated pressure drop and the experimental data are compared. The simulated results are also compared with the OPENFOAM results. The simulated results by the present model are in good agreement with the experimental data [32], and simulated results from OPENFOAM package [29] and are highlighted in Figure 5.5 and Figure 5.6 for different gas velocities at different L/G ratios.

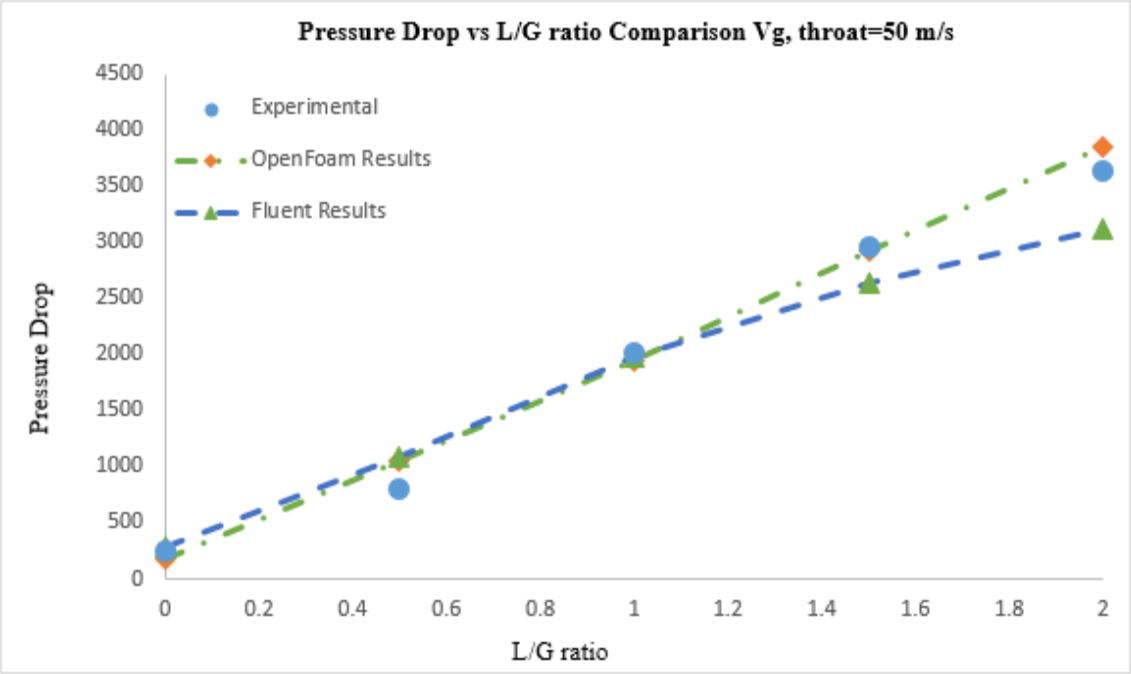


**Figure 5-5 Comparison of experimental data and simulation results for different L/G ratio at Vg, throat=50m/s**

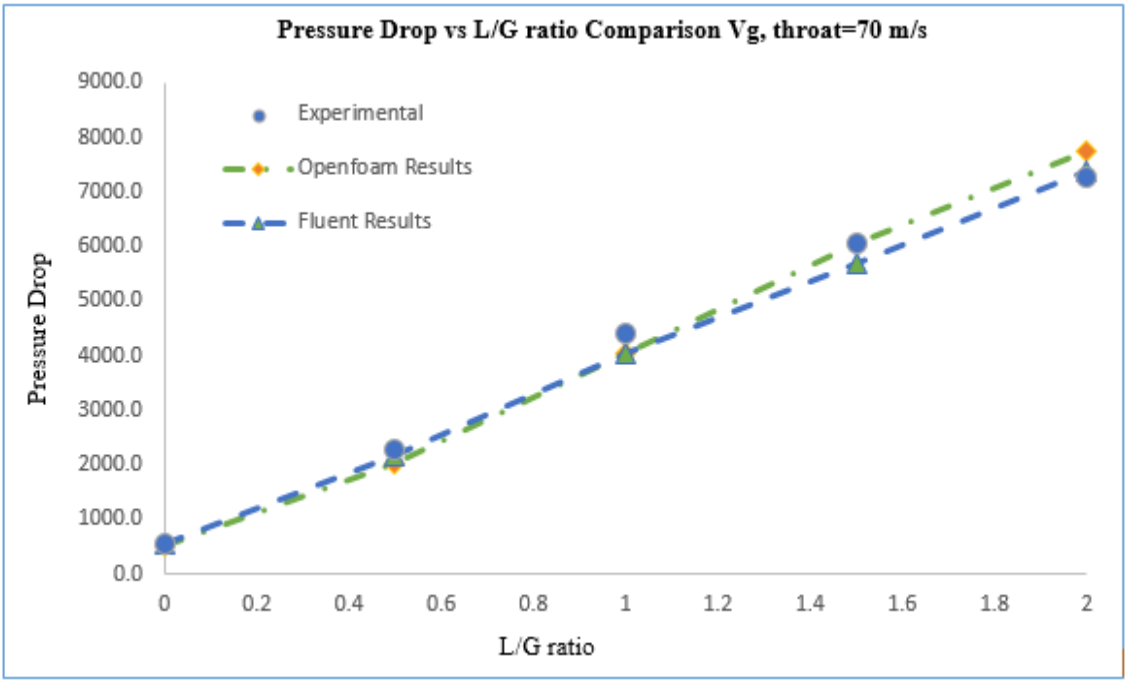


**Figure 5-6 Comparison of experimental data and simulation results for different L/G ratio at Vg, throat=70m/s**

The accuracy of the present simulation for the prediction of pressure drop is compared with the experimental data, and the relative error between the two is highlighted in Table 5.1 and Table 5.2.

**Table 5-1 Experimental and Simulated results comparison of Pressure drop for Vg, throat=50m/s at different L/G ratio**

| | **Present Model** | **Haller et al [32]** | |
|---|---|---|---|
| L/G ratio | Fluent Results | Model | % Error |
| **0** | 294 | 250 | 15 |
| **0.5** | 1094 | 800 | 27 |
| **1** | 1978 | 2025 | 2 |
| **1.5** | 2640 | 2955 | 11 |
| **2** | 3119 | 3645 | 14 |

**Table5-2 Experimental and Simulated results comparison of Pressure drop for Vg, throat= 70m/s at different L/G ratio**

| | **Present Model** | **Haller et al [32]** | |
|---|---|---|---|
| L/G ratio | Fluent Results | Model | % Error |
| 0 | 567.3 | 522.7 | 8 |
| 0.5 | 2282.7 | 2036.8 | 11 |
| 1 | 4427.5 | 4043.1 | 9 |
| 1.5 | 6079.9 | 6064.7 | 0.2 |
| 2 | 7286.8 | 7763.3 | 6 |

## 5.2 Droplet diameter

The droplet plays a significant role as a dust collector through inertial impaction mechanism in a venturi scrubber. Since the diameter of the droplet is directly related to the collection of the dust particles, the diameter of the droplet is investigated through this simulation. The droplet breakup phenomenon is modeled through the TAB model.

### 5.2.1 Gas velocity and L/G effect on Droplet size:

An increase in gas velocity generally decreases the droplet size. This can be explained by the fact that there should be a balance between the higher inertial forces and the surface forces through droplets of smaller size at higher throat gas velocities.

In the present work, water is introduced as a spray from plain orifice atomizer with a diameter of 2.5 mm. The increase in the liquid flow rates ultimately increases the injection velocity of the liquid. This results in the maximum contact between the incoming accelerated gas and injected droplets. The aerodynamic drag causes the droplet to break into smaller droplets thus resulting in the decrease of droplet diameter downstream of venturi. This behavior is highlighted graphically in Figure 5.7.

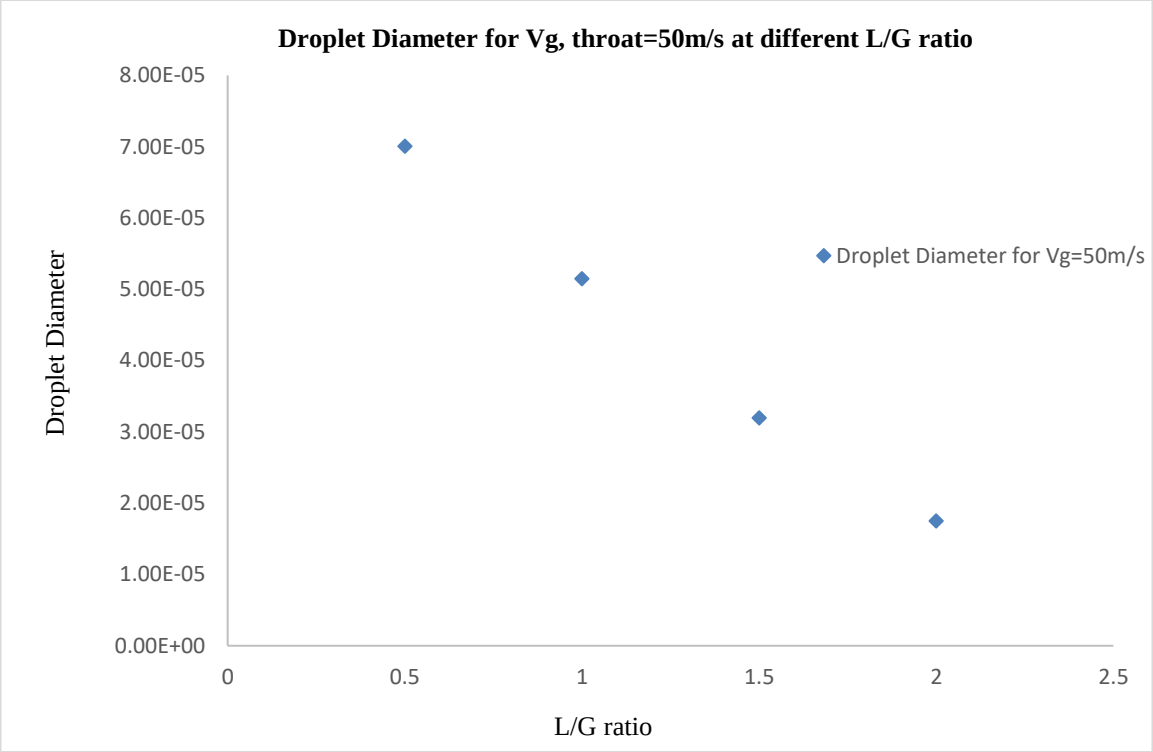


**Figure 5-7 Droplet Diameter for Vg, throat=50m/s at different L/G ratio**

## 5.3 Target Efficiency

Target efficiency or the impaction efficiency or the single droplet collection efficiency is also investigated in this research. The liquid is injected from a bank of nozzles located on the circumference of the throat. The target efficiency is calculated by using equation (3.24) and equation (3.25). The target efficiency is evaluated by investigating the effect of throat gas velocity and L/G ratio.

### 5.3.1 Throat Gas velocity effect on Target Efficiency

Throat gas velocity in this simulation is varied to observe its influence on the target efficiency. As the throat gas velocities increases, the momentum of the gas increase. This increase in momentum of the gas induces a strong drag force on the dust particles. Therefore the dust particles gain inertia at high throat velocity, and as a result, they are encapsulated in the droplets. The target efficiency for different throat gas velocities is shown in Figure 5.8.

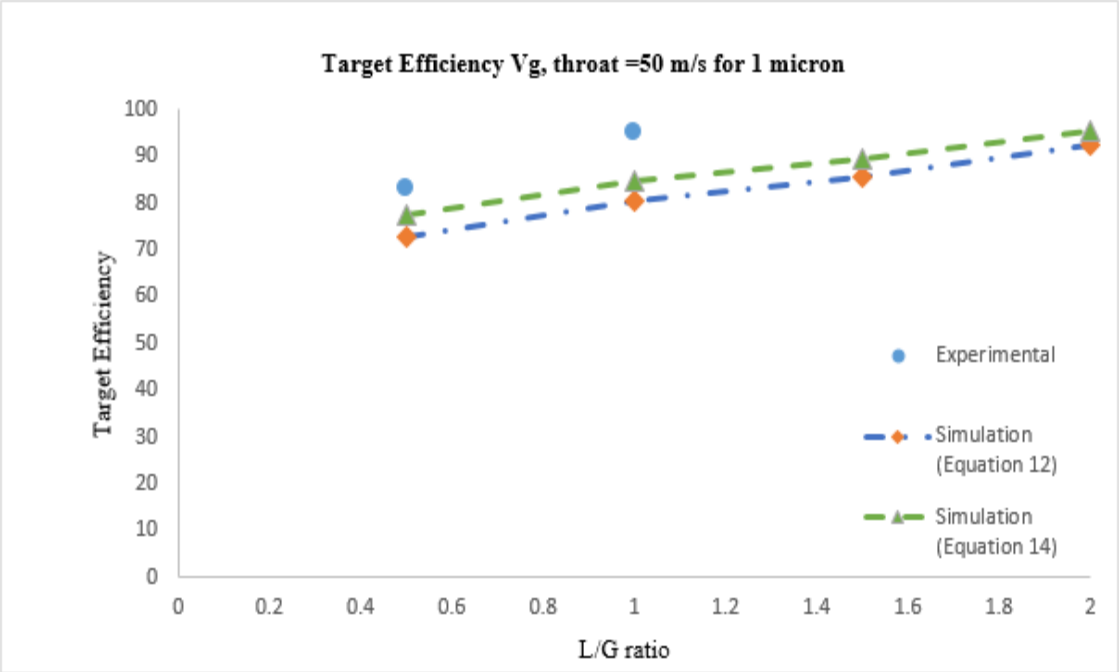


**Figure 5-8 Comparison of experimental and simulation results of target efficiency for Vg, throat=50m/s at different L/G ratio**

At higher throat gas velocities, the momentum transfer between the phases becomes more dominant and this results in the large relative velocities between the droplet and gas. This also enhances the phenomenon of the droplet breakup, and thus droplets of smaller diameter are produced. These smaller droplets will speed up the collection process of dust by droplets in the computational domain. The comparison of Experimental and simulated results for the throat gas velocity of 70 m/s is presented in Figure 5.9.

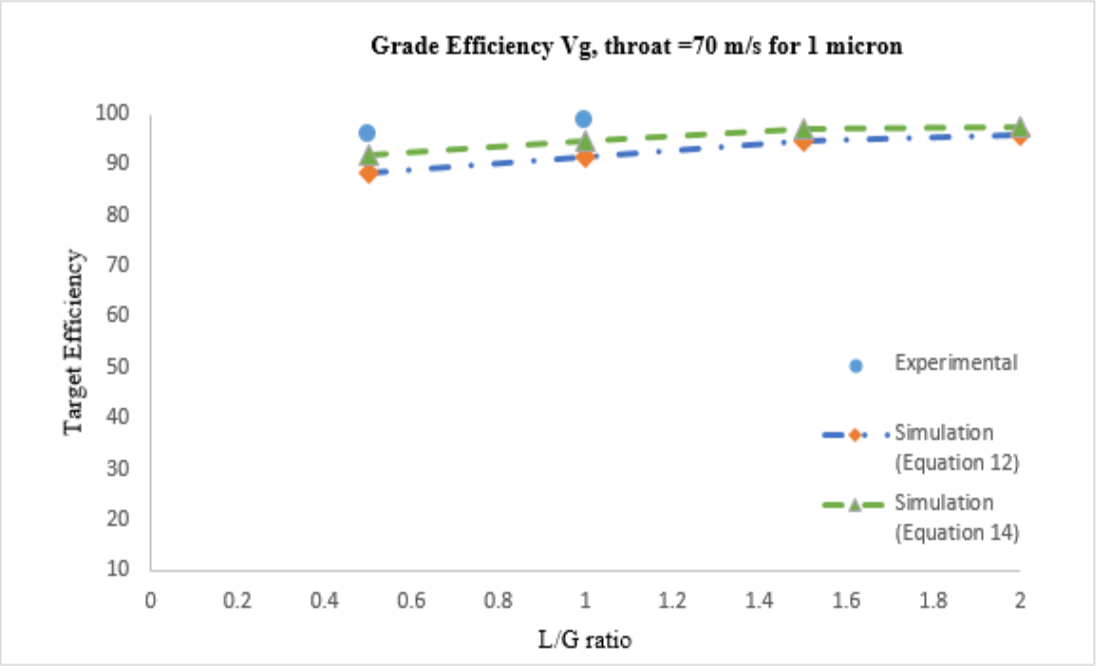


**Figure5-9 Comparison of experimental and simulation results of target efficiency for Vg, throat=70m/s at different L/G ratio**

### 5.3.2 Droplet Diameter effect on target efficiency

Droplet size and diameter is a paramount parameter as it function as dust collector. The droplet with small diameter will have large surface area, and thus it will act as a good collector for dust particle capturing. The prediction made by the present model for the collection efficiency is depicted in Figure 5.10.

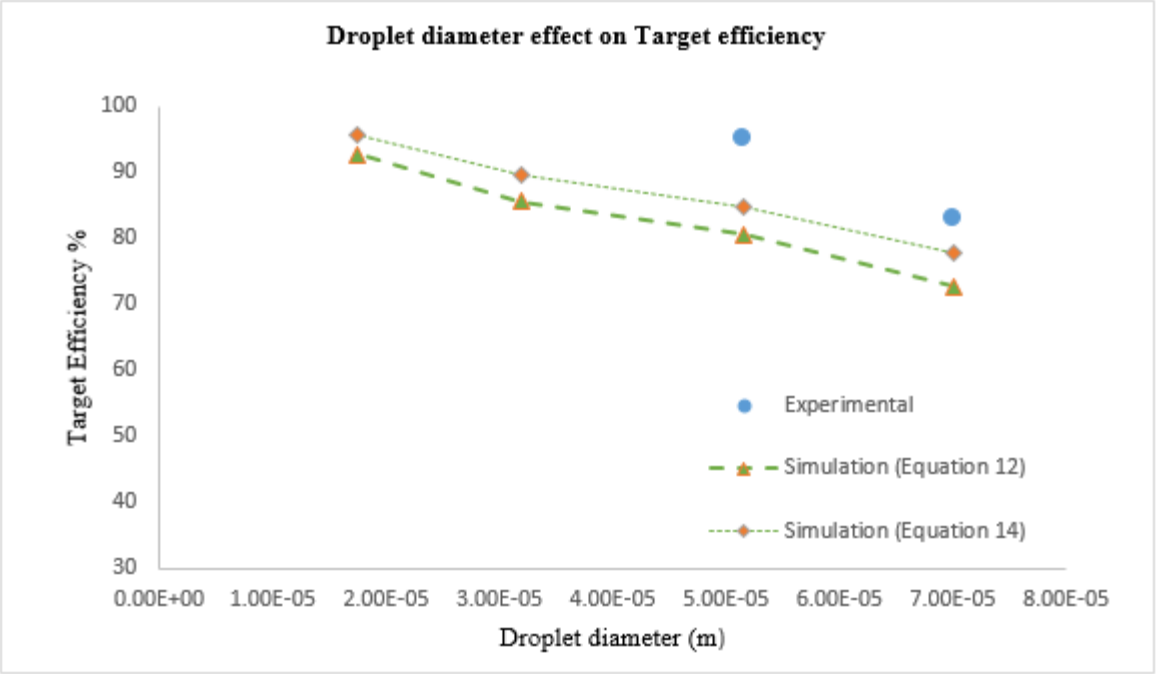


**Figure5-10 Comparison of experimental and simulation results of droplet diameter effect on target efficiency at Vg, throat=50m/s**

### 5.3.3 L/G ratio effect on Target Efficiency

L/G ratio is a critical design parameter which is studied to evaluate the performance of venturi scrubber. When liquid loading is increased for a given throat gas velocity, the target efficiency increases. This is due to the fact that by keeping L/G ratio high, the amount of droplets in the throat section increases and hence covers the whole throat. This throat coverage results in the maximum contact between the dust particles and the droplets thus enhance the target efficiency. The present model results agree well with the experimental data as highlighted in Figure 5.8 and Figure 5.9.

The present model calculates the target efficiency by using Calvert and Mohebbi model. It is concluded that the prediction made by the simulated results using Mohebbi equation (3.25) present less relative error as compared to results obtained using Calvert's equation (3.24). The results are highlighted in Table 5.3 and Table 5.4.

**Table 5-3 Comparison between simulation results and experimental data for target efficiency (Vg, throat=50 m/s) at different L/G ratio**

| | Haller [32] | Simulation results by equation 12 | | Simulation results by equation 14 | |
|---|---|---|---|---|---|
| L/G ratio | Experimental | Present model | % Error | Present model | % Error |
| 0.5 | 83 | 73 | 12 | 78 | 6 |
| 1 | 95 | 81 | 14 | 85 | 10 |
| 1.5 | - | 86 | - | 90 | - |
| 2 | - | 93 | - | 96 | - |

It is clear from the Table 5.3 and Table 5.4 that simulation results by using equation (2.9) is present less relative error and close to experimental data as compared to the simulation result obtained by using equation.

**Table5-4 Comparison between simulation results and experimental data for target efficiency (Vg, throat=70 m/s) at different L/G ratio**

| | Haller [32] | Simulation results by equation 12 | | Simulation results by equation 14 | |
|---|---|---|---|---|---|
| L/G ratio | Experimental | Calvert Equation | % Error | Mohebbi equation | % Error |
| 0.5 | 96 | 88 | 8 | 92 | 4 |
| 1 | 99 | 92 | 7 | 95 | 4 |
| 1.5 | - | 95 | - | 97 | - |
| 2 | - | 96 | - | 98 | - |

# Chapter-6

# Conclusion and Future Recommendations

A three-dimensional model is developed to study the performance estimation parameters i-e pressure drop and collection efficiency. The dispersed three phase Eulerian-Lagrangian model is simulated in ANSYS FLUENT. The turbulence of the system is computed through the realizable k-e model. TAB model was applied for the droplet breakup in the computational domain. Drag parameters are modeled by applying the spherical and dynamic drag laws. Target efficiency is calculated by Calvert and Mohebbi model.

The design parameters are evaluated at different throat gas velocities and L/G ratio. Pressure drop predicted by the present model agree well with the experimental data and model of Goniva. A little discrepancy in pressure drop is understood from the fact that the breakup constant in the TAB model is tuned by trial and error method which should be considered in future studies. Target efficiency from the present model using equation 3.24 and equation 3.25 is compared with experimental data. The target efficiency is little under predicted as compared to experimental data which can be referred to the droplet breakup and distribution. Moreover, it is concluded the relative error in prediction of collection efficiency by equation 3.25 is less as compared to Calvert equation. Overall the present model can be utilized for the optimization of the industrial scrubbers.

## Future Recommendations

Future work should focus on the following given topics to better predict the fluid dynamic behavior inside the venturi scrubber for its optimal performance:

a) CFD modeling of iodine removal from the exhaust gas with scrubber solution instead of water.

b) CFD modeling and simulation of simultaneous removal of dust and sulfur dioxide removal in a venturi scrubber.
c) CFD modeling of the film formation effect on venturi scrubber performance.

# References


[1] R. G. Holdich, *Fundamentals of particle technology*: Midland Information Technology and Publishing, 2002.

[2] R. Pulley, "Modelling the performance of venturi scrubbers," *Chemical Engineering Journal,* vol. 67, pp. 9-18, 1997.

[3] J. Gonçalves, D. F. Alonso, M. M. Costa, B. Azzopardi, and J. Coury, "Evaluation of the models available for the prediction of pressure drop in venturi scrubbers," *Journal of hazardous materials,* vol. 81, pp. 123-140, 2001.

[4] S. Calvert, "Venturi and other atomizing scrubbers efficiency and pressure drop," *AICHE journal,* vol. 16, pp. 392-396, 1970.

[5] R. H. Boll, "Particle collection and pressure drop in venturi scrubbers," *Industrial & Engineering Chemistry Fundamentals,* vol. 12, pp. 40-50, 1973.

[6] B. Azzopardi and A. Govan, "The modelling of venturi scrubbers," in *Filtech conference*, 1983, pp. 274-285.

[7] S. Calvert, D. Lundgren, and D. S. Mehta, "Venturi scrubber performance," *Journal of the Air Pollution Control Association,* vol. 22, pp. 529-532, 1972.

[8] S.-C. Yung, S. Calvert, and H. F. Barbarika, "Venturi scrubber performance model," *Environmental Science & Technology*, vol. 12, pp. 456-459, 1978.

[9] S. Pak and K. Chang, "Performance estimation of a Venturi scrubber using a computational model for capturing dust particles with liquid spray," *Journal of hazardous materials,* vol. 138, pp. 560-573, 2006.

[10] T. COLLINS, C. SEABORNE, and A. ANTHONY, "Removal of salt cake fume from sulphate recovery furnace stack gases by scrubbing," *Technical Association Papers*, vol. 30, pp. 168-172, 1947.

[11] H. Johnstone, R. Feild, and M. Tassler, "Gas absorption and aerosol collection in a venturi atomizer," *Industrial & Engineering Chemistry,* vol. 46, pp. 1601-1608, 1954.

[12] K. G. Hollands and K. C. Goel, "A general method for predicting pressure loss in venturi scrubbers," *Industrial & Engineering Chemistry Fundamentals,* vol. 14, pp. 16-22, 1975.

[13] M. Taheri and C. M. Sheih, "Mathematical modeling of atomizing scrubbers," *AIChE Journal,* vol. 21, pp. 153-157, 1975.

[14] T. Placek and L. Peters, "Analysis of particulate removal in venturi scrubbers—role of heat and mass transfer," *AIChE Journal,* vol. 28, pp. 31-39, 1982.

[15] S. Viswanathan, A. Gnyp, and C. St Pierre, "Annular flow pressure drop model for pease–anthony-type venturi scrubbers," *AIChE journal,* vol. 31, pp. 1947-1958, 1985.

[16] S. d. F. C. F. Teixeira, *A model for the hydrodynamics of venturis applicable to scrubbers,* 1989.

[17] B. Azzopardi, S. Teixeira, A. Govan, and T. Bott, "Improved model for pressure drop in venturi scrubbers," *Process Safety and Environmental Protection,* vol. 69, pp. 237-245, 1991.

[18] H. Sun and B. Azzopardi, "Modelling gas–liquid flow in venturi scrubbers at high pressure," *Process Safety and Environmental Protection,* vol. 81, pp. 250-256, 2003.

[19] A. Rahimi, A. Niksiar, and M. Mobasheri, "Considering roles of heat and mass transfer for increasing the ability of pressure drop models in venturi scrubbers," *Chemical Engineering and Processing: Process Intensification,* vol. 50, pp. 104-112, 2011.

[20] J.-S. Kim and J. W. Park, "Comparative Study on One-Dimensional Models for Particle Collection Efficiency of a Venturi Scrubber," 2016.

[21] A. A. Zerwas and J. L. de Paiva, "CFD SIMULATION OF TWO-PHASE FLOW IN A VENTURI SCRUBBER: VALIDATION AND COMPARISON OF SECONDARY ATOMIZATION MODELS," 2017.

[22] ANSYS. *ICEM CFD Help Manual ANSYS, Inc. Southpointe 2600 ANSYS Drive Canonsburg, PA 15317 USA.*

[23] L. Marocco and F. Inzoli, "Multiphase Euler–Lagrange CFD simulation applied to wet flue gas desulphurisation technology," *International Journal of Multiphase Flow*, vol. 35, pp. 185-194, 2009.

[24] F. Ahmadvand and M. Talaie, "CFD modeling of droplet dispersion in a Venturi scrubber," *Chemical Engineering Journal*, vol. 160, pp. 423-431, 2010.

[25] M. Ali, C. Q. Yan, Z. N. Sun, J. J. Wang, and A. Rasool, "CFD Simulation of Throat Pressure in Venturi Scrubber," in *Applied Mechanics and Materials*, 2012, pp. 3630-3634.

[26] M. Ali, C. Yan, Z. Sun, J. Wang, and H. Gu, "CFD simulation of dust particle removal efficiency of a venturi scrubber in CFX," *Nuclear Engineering and Design*, vol. 256, pp. 169-177, 2013.

[27] A. Sharifi and A. Mohebbi, "A combined CFD modeling with population balance equation to predict pressure drop in venturi scrubbers," *Research on Chemical Intermediates,* vol. 40, pp. 1021-1042, 2014.

[28] A. Mohebbi, M. Taheri, J. Fathikaljahi, and M. Talaie, "Simulation of an orifice scrubber performance based on Eulerian/Lagrangian method," *Journal of hazardous materials,* vol. 100, pp. 13-25, 2003.

[29] C. Goniva, Z. Tukovic, C. Feilmayr, T. Burgler, and S. Pirker, "Simulation of offgas scrubbing by a combined Eulerian-Lagrangian model," in *Seventh International Conference on CFD in the Minerals and Process Industries, CSIRO, Melbourne, Australia*, 2009, pp. 09-11.

[30] L. Tao and W. Kuisheng, "Numerical Simulation of Three-dimensional Heat and Mass Transfer in Spray Cooling of Converter Gas in a Venturi Scrubber," *CHINESE JOURNAL OF MECHANICAL ENGINEERING,* vol. 22, pp. 745-754, 2009.

[31] M. Ali, C. Yan, Z. Sun, H. Gu, and K. Mehboob, "Dust particle removal efficiency of a venturi scrubber," *Annals of Nuclear Energy,* vol. 54, pp. 178-183, 2013.

[32] H. Haller, E. Muschelknautz, and T. Schultz, "Venturi scrubber calculation and optimization," *Chemical engineering & technology,* vol. 12, pp. 188-195, 1989.

[33] C. T. Crowe, J. D. Schwarzkopf, M. Sommerfeld, and Y. Tsuji, *Multiphase flows with droplets and particles*: CRC press, 2011.

[34] D. S. A. Laari, "CFD simulation of two-phase and three-phase flows in internal-loop airlift reactors," Lappeenranta University of Technology, 2010.

[35] E. Stenmark, "On multiphase flow models in ANSYS CFD software," *Department of Applied Mechanics Division of Fluid Dynamics. Chalmers university of technology. Göteborg, Sweden,* vol. 75, 2013.

[36] ANSYS. *Fluent Theory Guide ANSYS, Inc. Southpointe 2600 ANSYS Drive Canonsburg, PA 15317 USA.* .

[37] P. J. O'Rourke and A. A. Amsden, "The TAB method for numerical calculation of spray droplet breakup," Los Alamos National Lab., NM (USA)1987.

[38] S. Morsi and A. Alexander, "An investigation of particle trajectories in two-phase flow systems," *Journal of Fluid mechanics,* vol. 55, pp. 193-208, 1972.